MECHANISMS OF T CELL MIGRATION TO VASCULARIZED ORGAN TRANSPLANTS

by

Jeffrey Walch

B.S.A, Carnegie Mellon University, 2002

Submitted to the Graduate Faculty of

School of Medicine in partial fulfillment

of the requirements for the degree of

Doctor of Philosophy

University of Pittsburgh

2013

UNIVERSITY OF PITTSBURGH

SCHOOL OF MEDICINE

This dissertation was presented

by

Jeffrey Walch

It was defended on

March 14th, 2013

and approved by

Fadi Lakkis, MD, Department of Surgery

Geetha Chalasani, MD, Department of Medicine

Pawel Kalinski, MD, PhD, Department of Surgery

Lawrence Kane, PhD, Department of Immunology

Eric Lagasse, PhD, Department of Pathology

MECHANISMS OF T CELL MIGRATION TO VASCULARIZED ORGAN TRANSPLANTS

Jeffrey Walch, PhD

University of Pittsburgh, 2013

A critical event in the rejection of transplanted organs is the migration of effector or memory T cells to the graft. The prevailing view is that the key steps involved in this process, integrin-mediated firm adhesion followed by transendothelial migration, are dependent on the activation of $G\alpha_i$-coupled chemokine receptors on T cells. In contrast to this view, we demonstrate *in vivo* that cognate antigen is necessary for the firm adhesion and transendothelial migration of $CD8^+$ effector T cells specific to graft antigens and that both steps occur independent of $G\alpha_i$ signaling. Presentation of cognate antigen by either graft endothelial cells or bone marrow derived antigen presenting cells that extend into the capillary lumen was sufficient for T cell migration. The adhesion and transmigration of antigen non-specific (bystander) effector T cells, on the other hand, remained dependent on $G\alpha_i$ but required the presence of antigen-specific effector T cells. These findings underscore the primary role of cognate antigen presented by either endothelial or bone marrow derived antigen-presenting cells in the migration of T cells across endothelial barriers and have important implications for the prevention and treatment of graft rejection.

TABLE OF CONTENTS

LIST OF FIGURES

PREFACE

This work would not be possible without the expertise and assistance of several talented individuals at the University of Pittsburgh: Dr. Fadi Lakkis, Dr. Martin Oberbarnscheidt, Dr. Geoffrey Camirand, Dr. Rosemary Hoffman, Dr. Qiang Zeng, Dr. Qi Li, Amanda Williams and Dr. Jiyun Kim. This dissertation and scientific findings detailed in the subsequent pages are dedicated to my friends and family who provided the love and support which helped with the completion of this project.

1.0 INTRODUCTION

1.1 OVERVIEW

Allograft rejection is caused by both naïve and memory T cells [1]. Naïve T cells encounter alloantigens in secondary lymphoid tissues where they differentiate into effector T cells – these in turn migrate to and reject the graft [2]. Memory T cells, in contrast, can initiate rejection by directly homing to the graft itself [3-5]. The prevailing view is that effector and memory T cell migration to vascularized organ transplants follows the classical leukocyte migration paradigm [6]. According to this paradigm, chemokines displayed on the inflamed endothelium engage $G\alpha_i$-coupled chemokine receptors on rolling T cells and trigger their firm adhesion and transmigration via integrin-dependent mechanisms [7]. Although blocking integrins has been shown to reduce T cell infiltration and delay graft rejection [8, 9], targeting individual or multiple chemokine receptors has had modest or no effects [10-12]. This prompted us to re-examine the role of $G\alpha_i$-coupled chemokine receptors in the migration of effector and memory T cells to vascularized organ transplants.

Using mouse models of heart and kidney transplantation and intravital high-resolution microscopy, we establish that T cell firm adhesion and transmigration across the graft endothelium is primarily driven by cognate antigen and not by $G\alpha_i$-dependent chemokine receptor signaling. Importantly, we demonstrate that the antigen presentation step required for T

cell migration is not restricted to endothelial cells but is also carried out by bone marrow derived antigen-presenting cells in the graft.

1.2 ROLE OF $CD8^+$ T CELLS IN ALLOGRAFT REJECTION

Naïve and memory T cells both play an important role in mediating the rejection of vascularized organ transplants [1]. Naïve T cells are exposed to alloantigens in secondary lymphoid tissues where they are primed to differentiate into effector T cells which in turn migrate to and reject the graft [2].

Alloreactive T cell recognition of allograft MHC antigen is the main precipitating event that eventually leads the rejection of vascularized organ transplants [13]. Alloreactive T cells are thought to recognize alloantigens through either the direct or indirect pathway [14]. In the "direct" pathway, intact donor major histocampatibilty complexes (MHC) with peptide are recognized directly by T cells on the surface of donor antigen presenting cells [15]. In the "indirect" pathway, recipient antigen presenting cells process donor MHC molecules and utilize self MHC to present this non-self peptide to recipient T cells [15]. However, experiments demonstrating that dendritic cells (DCs) are able to acquire and present functional MHCs from the surrounding microenvironment has led to the theory that $CD8^+$ T cells may be able to recognize alloantigen "directly" through the "semi-direct" pathway [16]. Therefore, although the specific mechanisms remain unclear, three different pathways have been proposed by which $CD8^+$ T cells recognize alloantigen (Figure 1) [15].

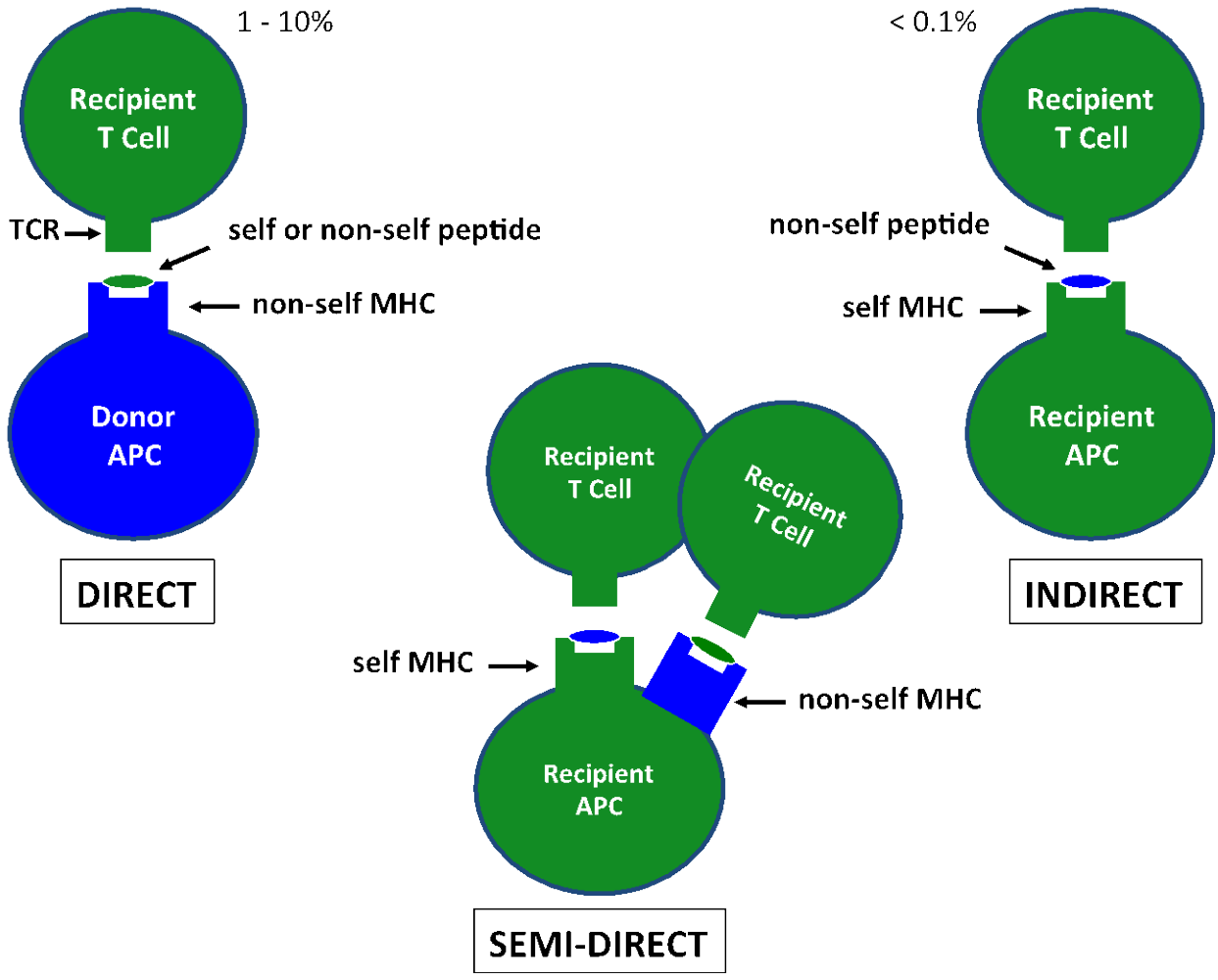

Figure 1. Pathways of alloantigen presentation.

The three pathways of alloantigen presentation (direct, indirect, and semi-direct) are shown. The frequency (%) of T cells that react to a specific pathway is indicated where known. APC: antigen presenting cell; MHC: major histocompatibility complex molecule; TCR: T cell receptor for antigen. Taken from: Kaplan et al, *Immunotherapy in Transplantation: Principles and Practice*, Wiley-Blackwell, 2012.

$CD8^+$ memory T cells are crucial players in the adaptive immune response that protects against infection [17] because of their long-term survival in humans [18] and rapid response to foreign antigen [19]. Unfortunately, due to a phenomenon known as heterologous immunity,

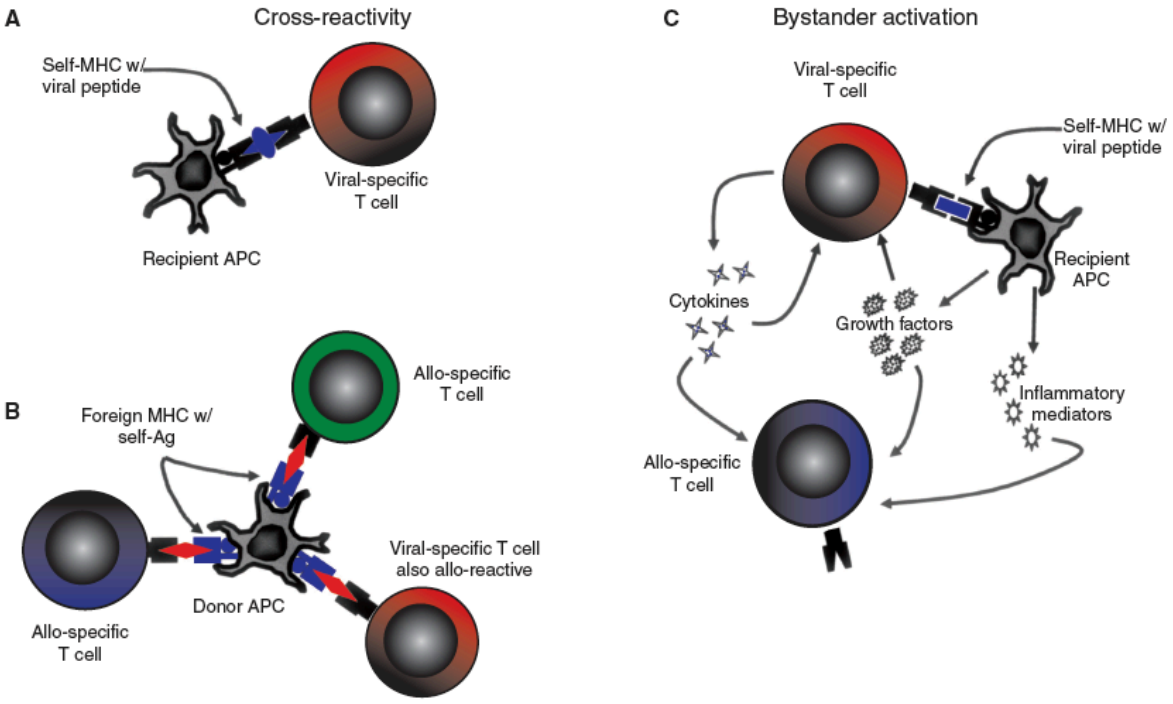

Figure 2. Heterologous immune response: cross-reactivity or bystander activation.

Previous immunological exposures can influence the course of future immune responses to unrelated stimuli, a phenomenon termed as heterologous immunity. This event may occur through at least two mechanisms: T-cell cross-reactivity or bystander activation. (**A**) The normal immune response to a pathogen, such as a virus, occurs when APCs process viral protein and present antigenic peptides complexed to self-major MHC molecules. (**B**) Unlike the standard immune response, the precursor frequency in alloreactivity can be as high as 1 in 10. A portion of the alloreactive repertoire may also recognize various antigens in the context of self-MHC. This 'molecular mimicry' occurs when a foreign MHC molecule containing self-peptide imitates the viral antigen complexed to self-MHC. (**C**) Alternatively, the heterologous response could occur through bystander activation, as viral-specific T cells release growth factors, cytokines, inflammatory mediators, etc., activating alloreative T cells in a non-specific manner. Taken from: Adams et al, *Heterologous Immunity: an overlooked barrier to tolerance*, Immunological Reviews, 2003.

$CD8^+$ memory T cells that are generated during immunological responses to infections (Figure 2, A) cross-react with donor allo-antigens (Figure 2, B) [20]. In addition to cross reactivity, alloreactive T cells could become activated in a non-specific manner by the release of inflammatory mediators from viral-specific T cells, a process known as bystander activation (Figure 2, C) [21]. Unlike naïve T cells, $CD8^+$ memory T cells have the ability to migrate directly from the bloodstream to reject allograft tissue without prior antigenic priming in lymphoid organs (Figure 3) [3]. Therefore, $CD8^+$ memory T cells are an important barrier to allograft survival and lead to the rejection of life saving organ transplants [22].

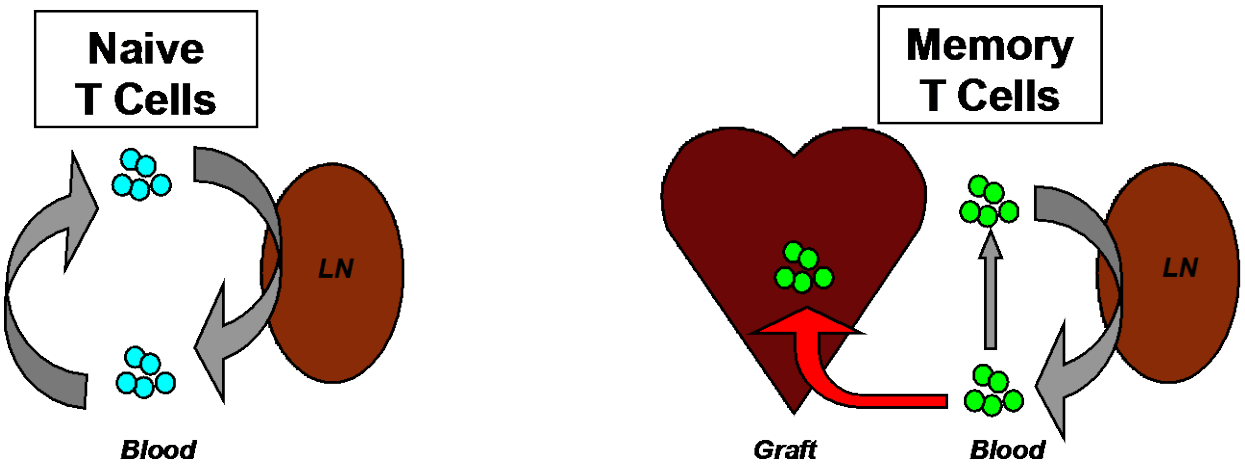

Figure 3. Memory T cells are able to migrate directly to the recipient's graft.

Unlike naïve T cells that require activation by antigen within secondary lymphoid tissue, $CD8^+$ memory T cells have the ability to migrate directly from the bloodstream to reject allograft tissue without prior antigenic priming in lymphoid organs.

Acute organ transplant rejection has been successfully reduced by treatment with immunosuppressive drugs [23]. However, side effects including renal toxicity, neurotoxicity and the induction of diabetes, limit the dosage that may be provided and the long-term effectiveness of treatment [24-26]. Furthermore, immunosuppressive therapy leads to an increased risk of infection and malignancy, affecting the over-all health of the patient [27]. The induction of donor-specific tolerance has consequently become a major goal in the field of transplantation research [28]. Although many tolerance induction strategies successfully target naïve T cells, memory T cells have proven to be a barrier [20].

Due to both the side effects of immunosuppressive drugs used for the prevention of allograft rejection [24-26] and the barriers to successful tolerance induction [20], developing novel treatment modalities to prevent the migration of $CD8^+$ effector or memory T cells to allograft tissue may prolong organ transplant survival. However, the signals and mechanisms involved in $CD8^+$ memory T cell migration to transplanted organs have not been determined.

1.3 TRANSENDOTHELIAL MIGRATION OF $CD8^+$ T CELLS

There is though to exist a common blood-borne pool of memory T cells, which possess broad migratory capability [29] and undergo transendothelial migration from the bloodstream to peripheral tissues in order to perform their role in immune surveillance, host defense and transplant rejection [3, 30]. Although the specific mechanism of $CD8^+$ memory T cell migration has not been determined, it is thought to operate under the paradigm of the leukocyte adhesion cascade: selectin mediated rolling, chemokine receptor activation, firm arrest due to binding of

high-affinity adhesion molecules to endothelial ligands, and subsequent transendothelial migration (Figure 4) [31]. Circulating leukocytes are thought to constitutively express low affinity adhesion molecules [32], which undergo conformational change to their high-affinity state after chemokine receptor signaling [33].

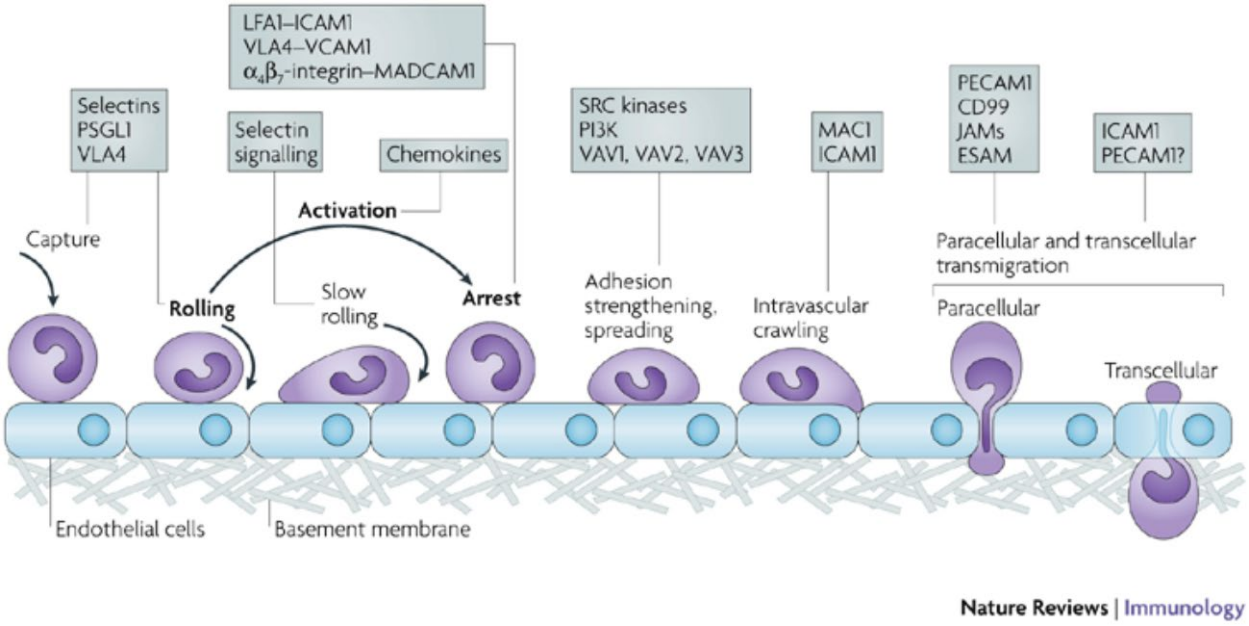

Figure 4. The updated leukocyte adhesion cascade.

The orginal three steps are shown in bold: rolling, which is mediated by selectins, activation, which is mediated by chemokines, and arrest, which is mediated by integrins. Progress has been made in defining additional steps: capture (or tethering), slow rolling, adhesion strengthening and spreading, intravascular crawling, and paracellular and transcellular transmigration. Key molecules involved in each step are indicated in boxes. Taken from: Ley et al, *Getting to the site of inflammation: the leukocyte adhesion cascade updated*, Nature Reviews Immunology, 2007.

1.4 THE ROLE OF CHEMOKINE RECEPTOR SIGNALING IN TRANSENDETHELIAL MIGRATION OF LEUKOCYTES

Chemokines presented by the endothelium bind specific G-protein coupled receptors (GPCRs) expressed on the surface of leukocytes and stimulate intracellular signaling, predominantly through the $G\alpha_i$ pathway, which is responsible for the firm arrest of leukocytes and their subsequent trans-endothelial migration [34]. Intracellular signaling modulates adhesion molecule function by two different methods [35]: (i) triggering the lateral mobility of adhesion molecules on the plasma membrane to form heterodimer clusters, known as clustering [36]; and (ii) stimulating conformational change of adhesion molecules to their high-affinity state [34]. Although lateral mobility clustering is involved [37], studies suggest that adhesion molecules must adopt their high-affinity conformation in order to facilitate the firm arrest and subsequent transendothelial migration of lymphocytes [7].

The migration of $CD8^+$ memory T cells to both the skin and the small intestine is dependent on chemokine receptor stimulation [38, 39]. Skin homing cells express adhesion molecule cutaneous lymphocyte antigen (CLA), as well as either chemokine receptor CCR10 or CCR4 [40, 41]. $CD8^+$ memory T cells that migrate to the small intestine express the integrin $\alpha4\beta7$ and the chemokine receptor CCR9 [42]. Genetic deletion of chemokine receptors CCR1, CCR5 or CXCR3 in the host resulted in reduced effector T cell accumulation in cardiac allografts and significantly delayed rejection [43-45]. Additional experiments examining effector T cells demonstrated that treatment with either anti-CCR5 or anti-CXCR3 monoclonal blocking antibodies prolonged allograft survival [43, 44].

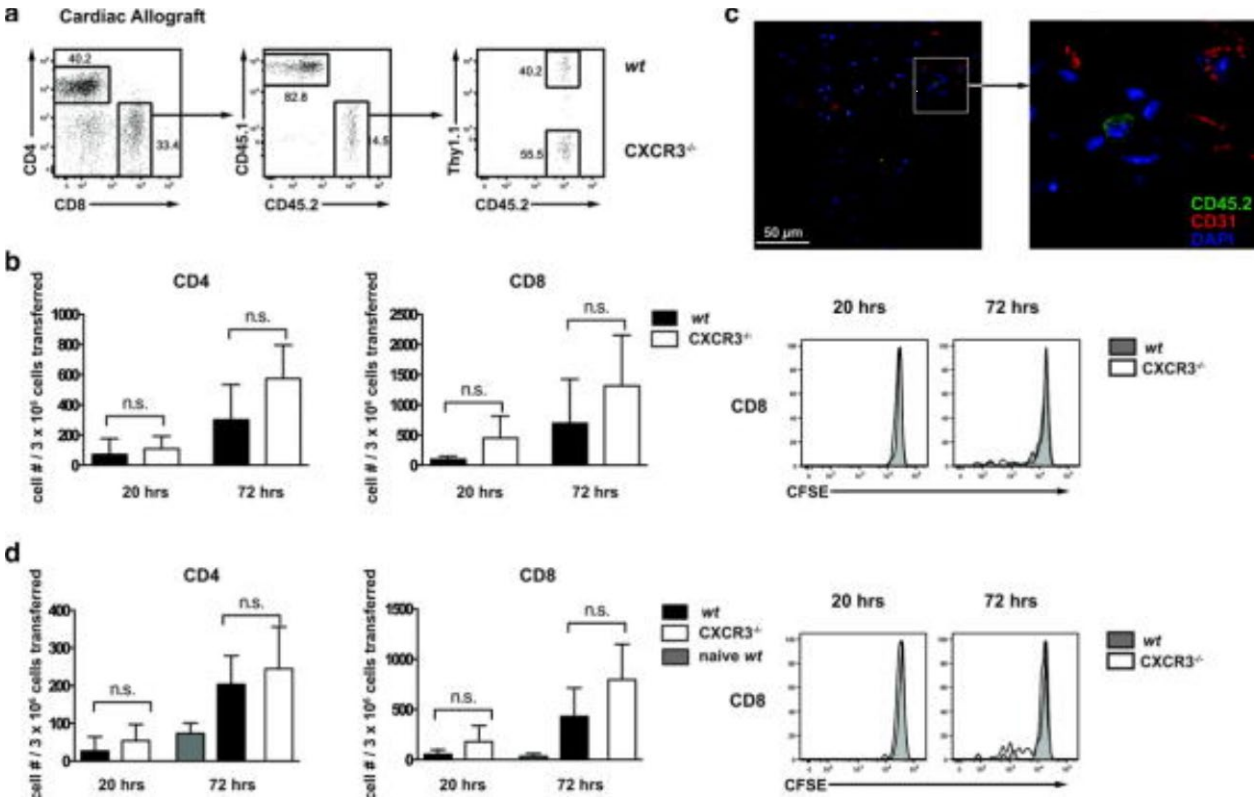

Figure 5. Memory T cells migrate to heart allografts independent of CXCR3 chemokine signaling.

Migration of wild type (WT) and CXCR3$^{-/-}$ memory T cells to cardiac allografts: Sorted WT (CD45.2, Thy1.1) and CXCR3$^{-/-}$ (CD45.2, Thy1.2) polyclonal CD4^{+} and CD8^{+} memory T cells were cotransferred to congenic (CD45.1, Thy1.2) recipients 2 days after cardiac allograft transplantation. Allografts were harvested at 20 and 72 hr after cell transfer. Cotransferred WT and CXCR3-/- memory T cells that infiltrated the graft were identified and quantitated by flow cytometry according to the gating strategy shown (**a**). (**b**) Quantitation of transferred WT and CXCR3-/- memory T cells recovered from allografts removed from WT recipients (two independent experiments; n=3 mice/experiment; mean+/-SD). Proliferation of recovered CD8 memory T-cell populations determined by CFSE dilution is shown in the histograms. (**c**) Immunofluorescence staining of cardiac allograft tissue demonstrating the presence of CXCR3-/- (CD45.2) memory T cells within the myocardium 6 days after transfer to congenic WT (CD45.1) recipients. Transferred T cells appear green (CD45.2+), endothelial cells red (CD31+), and nuclei blue (DAPI). White bar=50 [mu]m (magnification, x60). (**d**) Quantitation of transferred naive WT T cells and WT and CXCR3-/- memory T cells as described under (b) except that recipients were aly/aly-spleen mice (two independent experiments; n=3 mice/experiment; mean+/-SD). n.s.=not significant. Taken from: Oberbarnscheidt, Walch, et al, *Memory T cells migrate to and reject vascularized cardiac allografts independent of the chemokine receptor CXCR3*, Transplantation, 2011.

However, recent studies demonstrated that blocking recipient chemokine receptor CXCR3 had minimal impact on mouse cardiac allograft rejection [11]. In our investigation of the role of chemokines in memory T cell migration, we found that the migration of both $CD4^+$ and $CD8^+$ memory T cells to heart allografts occurs independent of CXCR3 chemokine receptor stimulated signaling (Figure 5) [12]. In addition, we demonstrated that cardiac allograft rejection by memory T cells is independent of CXCR3 and CCR5 chemokine signaling (Figure 6) [12]. Taken together these findings indicate that the role of chemokine receptor signaling, through the common $G\alpha_i$ pathway, in the migration of effector and memory T cells to vascularized organ transplants should be more thoroughly investigated.

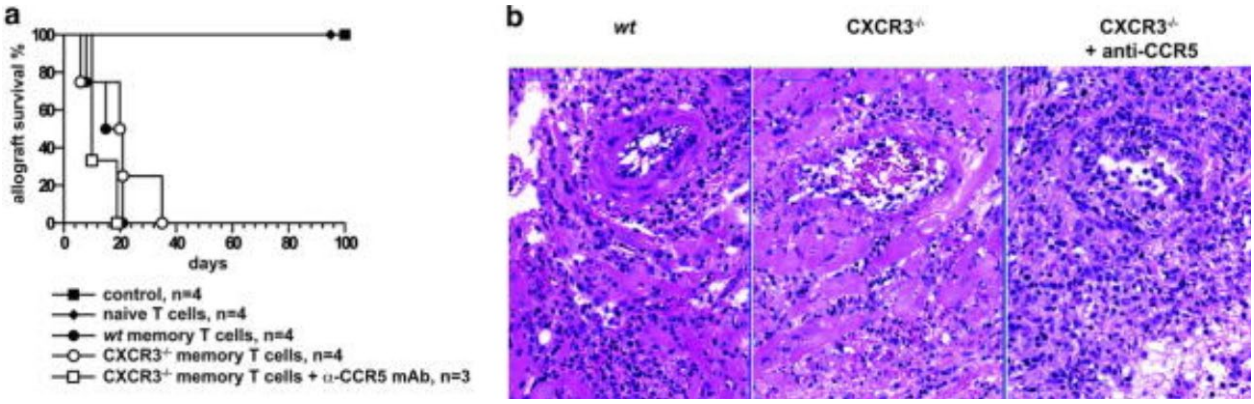

Figure 6. Cardiac allograft rejection by memory T cells is independent of CXCR3 and CCR5.

Cardiac allograft rejection by memory T cells is independent of CXCR3 and CCR5: $CD4^+$ and $CD8^+$ memory T cells were transferred to aly/aly-spleen recipients 2 days after cardiac transplantation and allograft survival was determined by palpation (a). Control mice did not receive any exogenous T cells or received naive T cells. Rat anti-mouse CCR5 antibody was administered daily for 15 days starting on the day before transplantation. No significant difference in allograft survival was observed among the groups that received memory T cells. (b) Representative cardiac allograft histology (hematoxylin-eosin staining) from the indicated groups showing extensive cellular infiltrate and myocyte destruction with active arteritis (magnification, x30). Taken from: Oberbarnscheidt, Walch, et al, *Memory T cells migrate to and reject vascularized cardiac allografts independent of the chemokine receptor CXCR3*, Transplantation, 2011.

1.5 CHEMOKINE INDEPENDENT MIGRATION OF T CELLS

Adhesion molecules expressed on the surface of T cells must adopt a high-affinity conformation, which may occur through chemokine stimulated $G\alpha_i$ signaling, in order to promote endothelial crawling and subsequent transendothelial migration [7]. Pertussis toxin (PTx) is a commonly used toxin that irreversibly blocks $G\alpha_i$ function and thereby inhibits chemokine-dependent T cell migration [46, 47]. Although the treatment of $CD8^+$ memory T cells with PTx prior to adoptive transfer into a (non-transplanted) mouse inhibited migration to the recipient's lymph nodes and peritoneal cavity, PTx treatment did not alter $CD8^+$ memory T cell migration to the recipient's bone marrow, lung or liver [48]. These results suggested that the migration of memory to T cells to select peripheral tissues, in a non-inflammatory microenvironment, may occur independent of chemokine signaling [48]. More specifically in a mechanistic sense, these results also suggest that the adhesion molecules on memory T cells may adopt a high-affinity conformation independent of endothelial chemokine stimulated signaling through the $G\alpha_i$ pathway.

Naïve T cells have been the predominant cell type utilized in the majority of *in-vivo* and *in-vitro* studies investigating the migration of lymphocytes to peripheral tissues, leading to the currently accepted paradigm for the leukocyte adhesion cascade [31]. However, the phenotype and function of naïve T cells differ dramatically from primed effector or memory T cell subpopulations [49]. The analysis of human $CD4^+$ memory T cells identified a subset that constitutively express the high-affinity VLA-4 integrin ($\alpha4\beta1$), prior to chemokine stimulation, which mediate high rates of initial attachment and firm arrest to VCAM-1 under flow conditions [50]. In comparison, human $CD4^+$ naïve T cells do not constitutively express high affinity VLA-4 and exhibit significantly lower accumulation on VCAM-1 enriched endothelium [50]. This

phenotypic difference in constitutive high-affinity adhesion molecule expression between $CD4^+$ memory and naïve T cell populations could explain some of the functional differences that have been observed between $CD8^+$ memory and naïve T cells.

Compared to naïve T cells, memory T cells are preferentially recruited to sites of inflammation and immune reactions [51]. Two-photon live tissue intravital imaging data has shown that $CD8^+$ memory T cells generated more frequent invasive filopodia and transmigrated more rapidly than their naïve counterparts [7]. Autoaggressive T cells, known as encephalitogenic T lymphoblasts, that initiate experimental autoimmune encephalomyelitis (EAE) in a mouse model, express an elevated level of high-affinity VLA-4 adhesion molecules that facilitate firm arrest to endothelial VCAM-1, without a requirement for chemokine-stimulated $G\alpha_i$ signaling [52]. Furthermore, the T lymphoblasts were captured independent of selectin mediated rolling [52]. This suggests a model in which constitutively expressed high-affinity VLA-4 is the exclusive receptor responsible for encephalitogenic T lymphoblast capture to the CNS blood vessel wall [53].

Murine peripheral blood T lymphocytes have also been shown to constitutively express a small subset of high affinity VLA-4 adhesion molecules that allow for firm arrest on endothelial VCAM-1, even in the absence of stimulatory chemokines [53]. IL-2 signaling, which is involved in the development of CD8 memory T cells [20, 54, 55], appears to trigger the induction of high-affinity VLA-4 integrin on circulating peripheral blood T lymphocytes in a chemokine independent fashion [56]. Additional studies demonstrated that the quantity of high-affinity VLA-4 is upregulated on T cells that are dependent on IL-2 [57]. More directly re-evaluating the leukocyte adhesion cascade in primed effector or memory T cells is necessary due

to the numerous phenotypic and functional differences between naïve and primed effector or memory T cells.

1.6 THE ROLE OF COGNATE ANTIGEN PRESENTATION IN THE MIGRATION OF T CELLS

Chemokine stimulated inside-out signaling through the $G\alpha_i$ pathway has been the major focus when investigating the mechanisms of leukocyte adhesion, as they pertain to migration of T cells to sites of inflammation or vascularized organ transplants. However, an alternative mechanism that may direct the migration of effector or memory T cells is the interaction of the T cell receptor (TCR) with cognate antigen presented by endothelial or tissue resident antigen-presenting cells (APC) [58-62]. Cognate antigen stimulation of the TCR triggers inside-out signaling, independent of the $G\alpha_i$ pathway [63, 64], which changes the conformation of integrins (namely, LFA-1 and VLA-4) from a low affinity to a high affinity ligand binding state (Figure 7) [63, 65, 66].

Intravital microscopy of the murine cremasteric vascular bed revealed that recognition of endogenously derived HY peptide on the endothelium enhanced the transendothelial migration of HY-specific T cells into the tissue [59]. However, this study did not investigate the specific roles of chemokine-stimulated $G\alpha_i$ signaling versus cognate antigen stimulation through the TCR on either the firm adhesion or transendothelial migration. An analysis of the early stages of a mouse autoimmune diabetes model found that diabetogenic $CD4^+$ T cells only infiltrated islets of

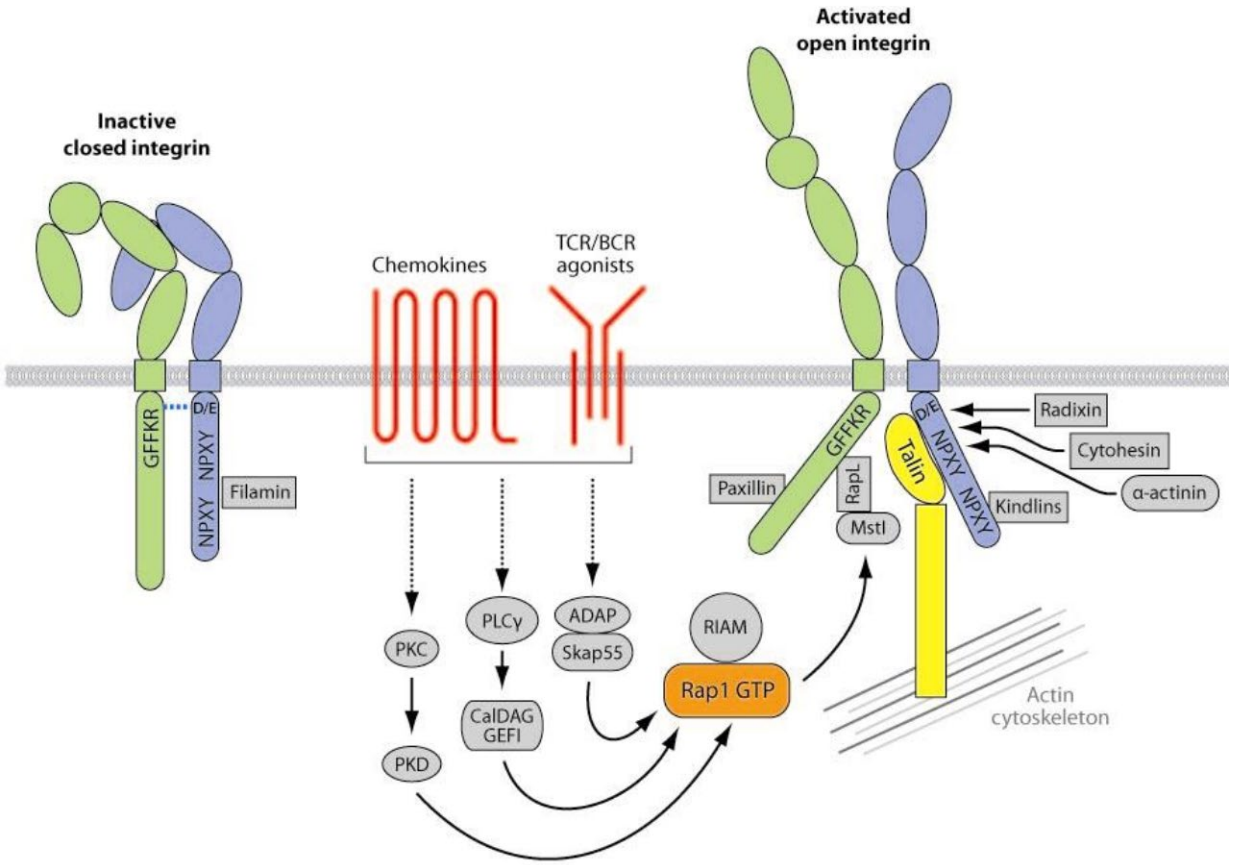

Abram CL, Lowell C. 2009.
Annu. Rev. Immunol. 27:339–62

Figure 7. Intergrin inside-out signaling.

The figure outlines the key signaling events that occur downstream of chemokine and T and B cell receptors that lead to integrin activation. Inactive integrins exist in a bent conformation, and the α and β cytoplasmic tails are held in close proximity by a salt bridge between residues found in the membrane-proximal region of the tail. Activation of a variety of signaling pathways results in the recruitment of GTP-bound Rap1 and activated talin to the integrin, leading to tail separation. The conformational change in the cytoplasmic region is transmitted through the integrin transmembrane domain and results in structural changes in the extracellular region, leading to an open conformation that can bind ligand with high affinity. The C-terminal rod domain of talin interacts with the actin cytoskeleton to provide physical coupling of the integrin to the actin network of the cell. Many other molecules interact with integrin cytoplasmic tails, but exactly how these interactions are coordinated with integrin activation is unclear. Taken from: Abram, et al, *The ins and outs of leukocyte integrin signaling*, Annual Review of Immunology, 2009.

Langerhans presenting their specific cognate antigen, and that this migration process occurred independent of chemokine stimulated the $G\alpha_i$ signaling [67, 68]. The infiltration of antigen specific diabetogenic $CD4^+$ T cells was required in order to induce the migration of non-specific $CD4^+$ T cells to the islets of Langerhans and initiate the development of murine autoimmune diabetes signaling [67, 68]. Dissecting the roles of chemokine-stimulated $G\alpha_i$ signaling and the presentation of cognate antigen on the migration of $CD8^+$ effector or memory T cells to vascularized organ transplants would provide specific details to be included in the paradigm of the leukocyte adhesion cascade.

1.7 TWO-PHOTON INTRAVITAL MICROSCOPY

Intravital microscopy is the most advantageous technique to utilize in order to determine the mechanistic details of T cell migration to vascularized organ transplants [69]. Immunofluorescence of histological tissue sections is a useful technique that provides a static analysis of cellular migration [12]. However, intravital microscopy facilitates the dynamic analysis of cellular morphology, interactions and motility parameters [70]. In regard to the leukocyte adhesion cascade, live *in vivo* imaging of graft tissue allows the visualization of specific steps including firm adhesion and transmigration [71].

Two-photon fluorescence occurs when two photons, of approximately the same energy, excite a fluorophore simultaneously [72]. The excitation level produced by the two photons together is equal to a single photon possessing twice the amount of energy [73]. Therefore, light from two photons together result in an excited molecule emitting fluorescence equivalent to that

caused by a single photon with half the wavelength (Figure 8) [73]. The longer infra-red (IR) wavelengths used in two-photon microscopy are advantageous for two reasons: (1) light scattering is decreased at longer wavelengths [74] and (2) biological tissues are considered optically transparent in the "optical window" from 700 to 900nm because of the minimal absorbance of light by water, lipids and hemoglobin within these higher wavelengths (Figure 9) [72]. The optical transparency of tissues to IR light allows two photon microscopes to penetrate tissues deeper than single photon confocal microscopes, up to 400μm in the lymph nodes as an example [75].

The other main advantage of two-photon microscopy over single-photon confocal microscopes is that excitation is confined exclusively to the focal plane (Figure 8) [76]. This limits the photobleaching and phototoxicity of a biological sample imaged by two-photon

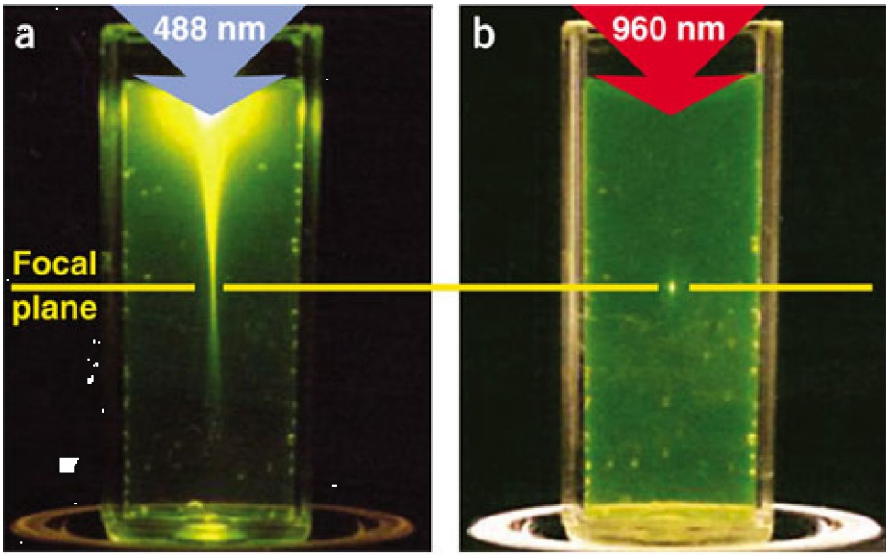

Figure 8. Localization of excitation by two-photon excitation.

(**a**) Single-photon excitation of fluorescein by focused 488-nm light (0.16 NA). (**b**) Two-photon excitation using focused (0.16 NA) femtosecond pulses of 960-nm light. Taken from: Zipfel, et al, *Nonlinear magic: multiphoton microscopy in the biosciences*, Nature Biotechnology, 2003.

microscopy to occur only at the focal plane [73]. Tissue damage is decreased by using two-photon microscopy because the generation of toxic byproducts of excitation, such as singlet oxygens and free radicals, is reduced [74]. Two-photon microscopy overcomes the limitations of single-photon confocal microscopy by reducing the amount of light scattering, photobleaching and phototoxicity.

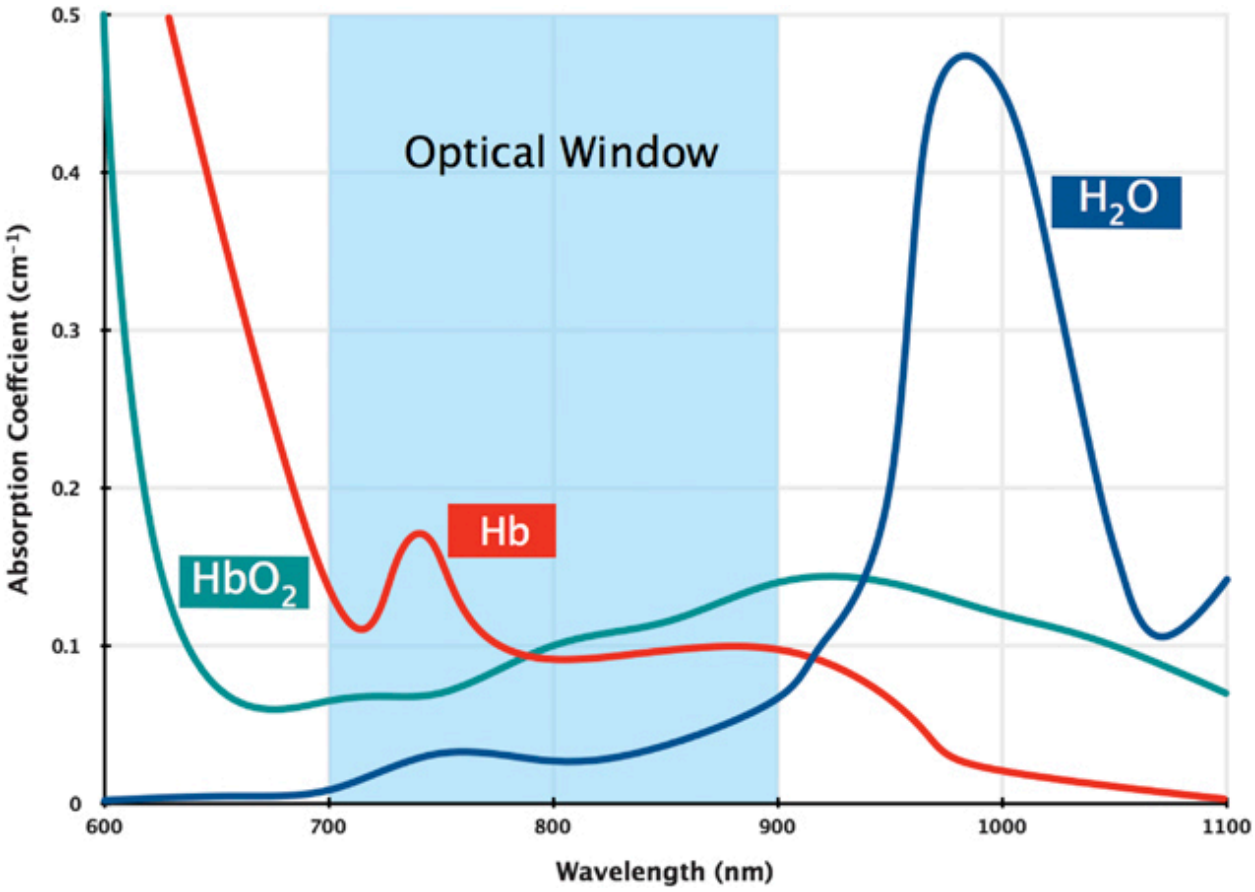

Figure 9. The absorption spectra of major tissue light absorbers haemoglobin and water.

In the 'optical window' between 700 and 900 nm there is little single-photon absorption (except by melanin that has a high absorption coefficient and may be present in lymph nodes and spleens of non-albino mice). Biological tissues are considered optically transparent in this commonly used imaging window.- Taken from: Phan, et al, *Practical intravital two-photon microscopy for immunological research: faster, brighter, deeper*, Immunology & Cell Biology, 2010.

Two-photon microscopy is regarded as the gold standard methodology for intravital imaging analysis of living animals in minimally invasive fashion [77]. Two-photon microscopy has been utilized to analyze the dynamic cellular interactions of lymphocytes in the murine lungs [78], lymphoid organs [79], and the central nervous system [80]. Additionally, our laboratory

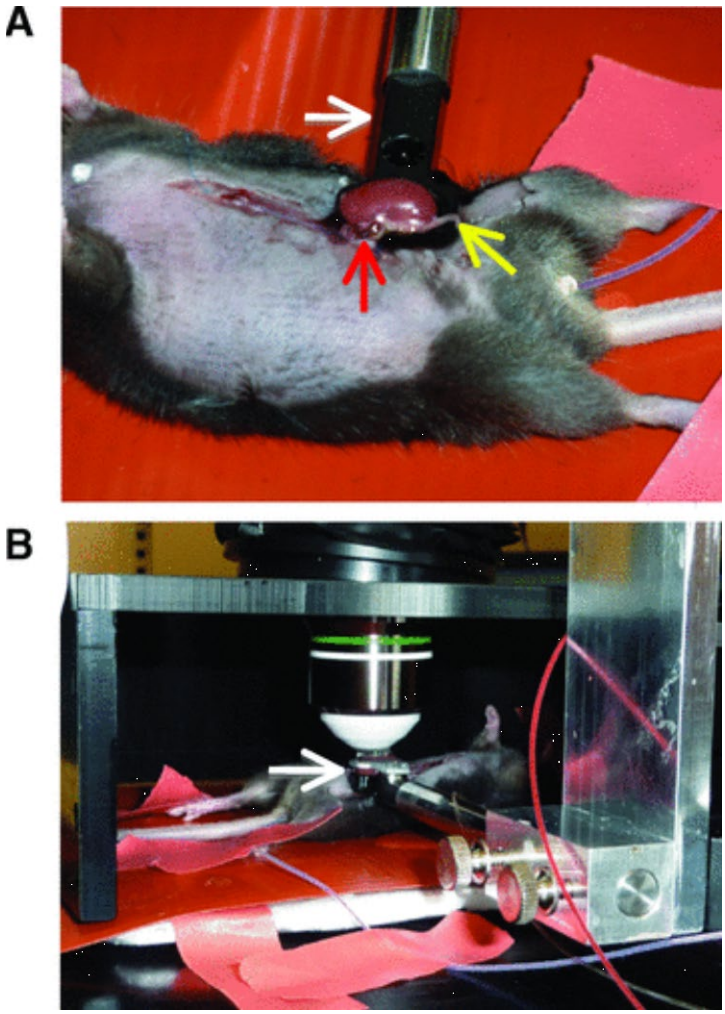

Figure 10. Setup for two-photon microscopy of the transplanted mouse kidney.

(**A**) Renal graft in imaging cup and holder arm (white arrow) before placement of cover slip. Note vascular pedicle (red arrow) and exposed ureter (yellow arrow). (**B**) Anaesthetized mouse with renal graft immobilized in imaging cup (white arrow) under objective lens of upright microscope. Taken from: Camirand, et al, *Multiphoton Intravital Microscopy of the Transplanted Mouse Kidney*, American Journal of Transplantation, 2011.

established a procedure to perform two-photon intravital microscopy of the transplanted mouse kidney (Figure 10) [69]. Two-photon intravital microscopy is the ideal existing methodology to investigate the specific steps of the leukocyte adhesion cascade as it pertains to the migration of effector and memory T cells to vascularized organ transplants.

1.8 CLINICAL RELEVANCE

The central paradigm of the leukocyte adhesion cascade is that chemokine stimulated signaling through the $G\alpha_i$ pathway is required for the firm arrest of leukocytes and their subsequent trans-endothelial migration into tissues [34]. Early experiments involving effector T cells demonstrated that treatment with either anti-CCR5 or anti-CXCR3 monoclonal blocking antibodies prolonged allograft survival [43, 44]. However, recent studies have failed to confirm a necessary role for these chemokine receptors in rejection of vascularized organ transplants [11]. On the other hand, blockade of VLA-4 leads to cardiac allograft prolongation and possible long-term acceptance [81]. However, perhaps due to diminished immunosurveillance, the treatment of patients with monoclonal antibodies against VLA-4 has been associated with the development of progressive multifocal leukoencephalopathy (PML), which is a deadly demyelinating disease of the white matter in the brain [82]. Therefore, understanding the specific roles of chemokine stimulation and cognate antigen recognition in the firm adhesion and transmigration of effector or memory T cells to vascularized allografts may provide an additional therapeutic targets that could be utilized to prolong the survival of life saving organ transplants.

2.0 METHODS

2.1 MICE

C57BL/6J (B6) (Thy1.2, CD45.2, H-2^b), B6.PL-Thy1a/CyJ (Thy1.1, CD45.2, H-2^b), BALB/cJ (BALB/c) (H-2^d), C57BL/6J-Tg(CAG-OVA)916Jen/J (CD45.2, H-2^b) (B6-OVA), C57BL/6-Tg(TcraTcrb)1100Mjb/J (CD45.2, H-2^b) (OT-I), and B6 CD11c-YFP mice were purchased from The Jackson Laboratory (Bar Harbor, ME). B6.Cg-$Tcra^{tm1Mom}$ Tg(TcrLCMV)327Sdz (P14) mice (CD45.2, H-2^b) and B6 $H2Kb^{-/-}$ were purchased from Taconic (Germantown, NY). B6 $OVA^+CD11c\text{-}YFP^+$ mice and $OVA^+H2Kb^{-/-}$ mice were generated by cross breeding B6-OVA mice with either B6 CD11c-YFP or B6-$H2Kb^{-/-}$ mice respectively. H2kB6-Ly5.2/Cr (Thy1.2, CD45.1, H-2^b) were purchased from National Cancer Institute (NCI). OT-I mice were bred onto the $Rag^{-/-}$Thy1.1 and $Rag^{-/-}$Thy1.2 backgrounds. Alymphoplasia mice (Map3k14$^{aly/aly}$, Thy1.2, H-2^b) (*aly/aly*) were purchased from CLEA (Osaka, Japan) and bred onto a B6 CD45.1 congenic background. All animals were maintained under SPF conditions.

2.2 SURGICAL PROCEDURES AND BONE MARROW CHIMERAS

Splenectomies and heterotopic transplantation of vascularized heart and kidney grafts were performed as previously described [2, 69, 83]. Heart graft rejection was defined as cessation of

palpable heartbeat and was confirmed by histological analysis. Bone marrow chimeras were generated by irradiating recipient mice with 1000cGy from a Nordion Gamma Cell 40 cesium source. After irradiation the mice were injected retro-orbitally with 1 x 10^7 donor bone marrow cells. After an 8-week reconstitution period, blood was phenotyped to verify appropriate reconstitution. Chimerism was consistently greater than 90 – 95% in the blood and was confirmed in selected kidneys.

2.3 GENERATION, ISOLATION, AND ADOPTIVE TRANSFER OF EFFECTOR AND MEMORY T CELLS

2.3.1 Polyclonal Cells.

Polyclonal $CD4^+$ and $CD8^+$ effector and memory T cells were generated as described [12]. Briefly, B6 (CD45.2) mice on the Thy1.1 and Thy1.2 backgrounds were immunized i.p. with 2 x 10^7 BALB/c splenocytes on days 0 and 21. One or 6-8 wks after the first immunization, spleen and lymph node cells were harvested to obtain effector and memory T cells, respectively, and enriched for T cells by negative selection, labeled with carboxyfluorescein diacetate succinimidyl ester (CFSE) (Invitrogen), treated or not with 200 ng/ml pertussis toxin (PTx) (Sigma) for 30 minutes at 37° C (5% CO_2), and $CD44^{high}CFSE^+$ $CD4^+$ and $CD8^+$ effector and memory T cells were sorted on a BD Aria Plus high-speed sorter (purity ~95%). To study migration, equal numbers of PTx treated (Thy1.1, CD45.2) and untreated (Thy1.2, CD45.2) $CD4^+$ and $CD8^+$ effector or memory T cells (2-3 x 10^6 each) were co-transferred i.v. into B6

(Thy1.2, CD45.1) or splenectomized *aly/aly* (*aly/aly*-spleen, Thy1.2, CD45.1) recipients of BALB/c heart allografts. To study allograft rejection, the same number of PTx treated or untreated memory T cells were transferred separately into *aly/aly*-spleen recipients.

2.3.2 Monoclonal (TCR-tg) cells.

Dendritic cells (DC) were generated by culturing bone marrow cells with IL-4 and GM-CSF (Peprotech) for 8 days. DC were stimulated with 100 ng/ml LPS overnight and pulsed with either 10 □g/ml OVA for 2 hours at 37° C. 2-3 x 10^6 OVA or LCMV peptide-pulsed DC were injected i.v. with 5 x 10^5 OT-I (Thy1.1, CD45.2) or P14 (Thy1.2, CD45.2) T cells, respectively, into B6 (Thy1.2, CD45.1) mice based on published method [84]. Five days later, spleen and lymph node cells were labeled with CFSE, treated with PTx or not, and OT-1 and P14 effectors recovered by high-speed sorting $CD45.2^+CD8^+CFSE^+$ cells. Flow analysis confirmed that > 95% of these cells were $CD44^{high}$ and were OVA or LCMV MHCI-tetramer positive (Beckman-Coulter). OT-I and/or P14 effectors, with or without PTx treatment, were then co-transferred i.v. (1-2 x 10^6 each) into B6 (Thy1.2, CD45.1) recipients of either B6-OVA or B6 heart grafts.

To study the role of VLA-4 in migration, OT-I effector T cells were incubated prior to transfer with 100 μg/ml monoclonal rat anti-mouse VLA-4 antibody (PS/2, BioXCell) on ice for 20 minutes. In addition, recipients received 250 μg PS/2 i.p. on the day of cell transfer, and 1 and 2 days later.

For the intravital imaging studies, cells were labeled prior to transfer with 2 □M CFSE, cell tracker orange (CTO), or cell tracker violet (CTV) (Invitrogen) and high-speed sorted by

gating on $CD45.2^+CFSE^+/CTO^+/CTV^+$ cells and using the following dump channel: $CD4^+CD45R/B220^+CD11c^+CD11b^+CD49b^+Ly\text{-}76^+CD16/32^+F4/80^+$. Flow analysis confirmed that sorted populations were > 95% $CD8^+CD44^+$ and were tetramer positive. OT-I and/or P14 effectors, with or without PTx treatment, were then co-transferred i.v. (7-10 x 10^6 each) into B6 (Thy1.2, CD45.1) recipients of either a B6-OVA, B6 or chimeric kidney grafts.

2.4 ANALYSIS OF CELL MIGRATION BY FLOW CYTOMETRY

Heart grafts, kidney grafts, spleen, and lymph nodes were harvested at the indicated time points after T cell transfer. Lymphocytes were isolated from heart and kidney grafts as previously described [12]. Total number of recovered lymphocytes was determined and the transferred polyclonal and monoclonal T cells enumerated by flow cytometry by gating on the $CD45.2^+Thy1.1^+$ and $CD45.2^+Thy1.2^+$ populations after live/dead cell discrimination and exclusion of non-T cells ($CD45R/B220^+CD11c^+CD11b^+CD49b^+Ly\text{-}76^+CD16/32^+$ $F4/80^+$ cells). All fluorochrome- or biotin-tagged antibodies were purchased from BD Pharmingen, eBioscience, Biolegend, or R&D Systems: BDCD90.1 (OX-7), CD90.2 (30-H12), CD45.2 (104), CD45.1 (A20), CD8 (53-6.7), CD4 (RM4-5), CD44 (IM7), CD62L (MEL-14), CD45R/B220 (RA3-6B2), CD11c (HL3), CD11b (M1/70), CD49b (DX5), Ly-76 (TER-119), CD16/32 (2.4G2), and F4/80 (BM8). Fixable live/dead Aqua cell stain (405nm excitation) was purchased from Invitrogen. Flow acquisition was performed on LSRII and LSRFortessa analyzers (BD Biosciences), and data analyzed using Flowjo software (Treestar Corp.).

2.5 INTRACELLULAR CYTOKINE STAINING

OT-I and P14 effector T cells were cultured overnight with B6 splenocytes in the presence of 5 μg/mL of SIINFEKL or KAVYNFATM peptides respectively with Brefeldin A (eBioscience). Cells were stained for surface markers and then fixed/permeabilized (BD cytofix/cytoperm). Cells were then stained with IFNγ (XMG1.2, eBioscience) or isotype control.

2.6 MUTLI-PHOTON INTRAVITAL MICROSCOPY AND IMAGE ANALYSIS

Multi-photon intravital microscopy was performed on transplanted kidneys using an established method [69]. An Olympus FluoView FV1000 microscope with a Mai Tai DeepSee femtosecond-pulsed laser (Spectra-Physics), tuned and mode-locked to either 825nm or 860nm, was used for all experiments. The recipient mouse was anesthetized with isoflurane and oxygen and placed on a heating pad to maintain core body temperature at 37°C. An i.v. line was inserted in the external jugular vein to provide 5% dextrose lactated ringer's solution for hydration and 500kDa dextran conjugated with either FITC or Rhodamine for visualization of blood vessels in the transplanted kidney. The kidney graft was extraverted from the abdominal cavity with intact vascular connection and immobilized in a custom cup mount [69]. A coverslip was placed on top of kidney and z-stacks were visualized with a 25x water immersion objective (SP1 NA:1.05) 25 μm to 55 μm below the kidney capsule. 12 slices were acquired at a step size of 2.7 μm. Brightness and laser power were adjusted based on the imaging depth and kept below phototoxic levels. Dwell time was set to 8 μs/pixel and resolution was a maximum of 512 x 512. The

scanning area was cropped to adjust for a 30 second-long stack that was then repeatedly scanned up to 60 times for a maximum imaging time of 30 minutes per location. These settings were repeated up to five locations per transplanted kidney. T cells were enumerated at seven independent time points per z-stack.

Volocity software (Perkin-Elmer) was utilized to analyze acquired movies. Drift was corrected using the blood vessels as a reference point. Cells present in the field of view for at least five time points (> 2 min) were tracked in the *x*, *y*, and *z* direction for the duration of each video. Cells were determined to have firmly adhered if they were arrested for >30 sec in the capillary lumen and transmigrated if the majority or all of the cell body had moved outside the capillary lumen at any time during the course of their tracking. The motility parameters were plotted using Volocity.

2.7 IN-VITRO MIGRATION ASSAY

5μm pore size chemotaxis assay chamber (Millipore) was utilized with or without 0.5 □g/ml IP 10 in medium in the bottom chamber. $5x10^4$ OT-I effector T cells, isolated as described above, with or without pre-treatment with PTx were placed in the top chamber of each well for a total of 7-12 wells per group. The chamber was incubated at 37° C for 3 hrs after which the cells in the bottom chamber were collected and counted using a hemocytometer and trypan blue exclusion. The assay was repeated using OT-I effector T cells re-stimulated with SIINFEKL-pulsed DCs at 37°C for two hours prior to use in the chemotaxis assay. This restimulation protocol was sufficient to induce IFNγ production in 60% of the cells.

2.8 STATISTICAL METHODS

Statistical analysis of allograft survival was calculated using the log-rank test. All other experiments were analyzed using unpaired *t* test (2-tailed) for samples with normal distribution and the Mann-Whitney test (2-tailed) for samples with a non-Gaussian distribution. All statistical calculations were made in *GraphPad Prism 5.0c*. Significance was set at $P<0.05$.

2.9 STUDY APPROVAL

All animal studies were approved by the University of Pittsburgh IACUC, Protocol# 12050385, PHS assurance # A3187-01.

3.0 RESULTS

3.1 $CD8^+$ T CELLS MIGRATE TO HEART ALLOGRAFTS INDEPENDENT OF $G\alpha_I$ SIGNALING

To investigate whether $G\alpha_i$-dependent chemokine receptor signaling in T cells is required for their migration to vascularized organ grafts, we transplanted BALB/c (H-2d) heart allografts into B6 (H-2b) mice and two days later co-transferred pertussis toxin (PTx)-treated and untreated $CD4^+$ and $CD8^+$ memory or effector ($CD44^{high}$) T cells from B6 mice immunized with BALB/c splenocytes. PTx ADP-ribosylates $G\alpha_i$ proteins, irreversibly blocking $G\alpha_i$ mediated signal transduction and thereby inhibiting chemokine-dependent T cell migration [46, 47].

Grafts were removed 1, 3, and 6 days after cell transfer and the transferred $CD8^+$ T cells were identified by flow cytometry using congenic markers. Comparable numbers of PTx-treated and untreated $CD8^+$ memory T cells were present in the grafts on days 1, 3, and 6 after transfer and the two cell populations proliferated equally, progressing from no division on day 1 to > 8 divisions by day 6 (Figure 11). Results similar to those in Figure 11 were obtained when memory T cells were transferred to splenectomized alymphoplastic (*aly*/*aly*) mice lacking secondary lymphoid tissues due to an autosomal recessive mutation that causes a deficiency in the systemic lymph nodes (Figure 12), indicating that PTx-treated $CD8^+$ memory T cells migrate to the grafts

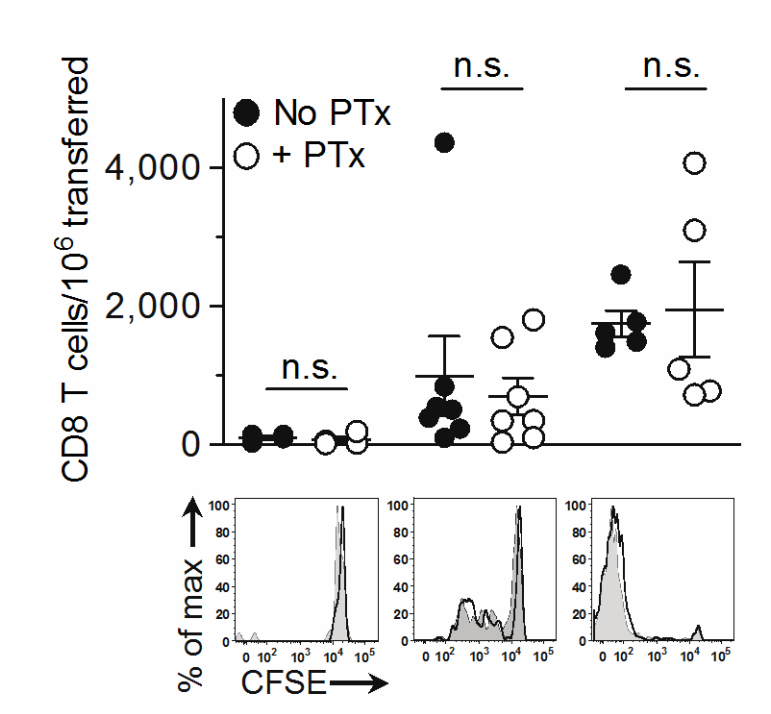

Figure 11. Gα_i-independent migration of memory T cells to heart allografts.

PTx-treated and untreated T cells were co-transferred into recipients of BALB/c cardiac allografts 2 days after transplantation. Graph depicts enumeration of transferred memory $CD8^+$ T cells in the graft on day one, three and six after cell transfer. T cell proliferation for co-transferred cells treated with PTx (black outline) and untreated (grey) is shown in the CFSE histograms. Results are mean ± s.e.m.; n.s. = not significant.

without first proliferating in secondary lymphoid tissues. Likewise, equal numbers of PTx-treated and untreated $CD8^+$ memory T cells infiltrated allografts allowed to heal for 50 days in splenectomized *aly*/*aly* recipients (Figure 13), suggesting that acute graft inflammation is not a pre-requisite for T cell migration.

Migration of T cells to the lymph nodes is directed by a Gα_i-dependent signaling process [85]. Therefore, the significantly diminished migration of PTx-treated T cells to the lymph nodes, as compared to untreated cells, confirmed that chemokine stimulated Gα_i signaling was blocked in these cells (Figure 14).

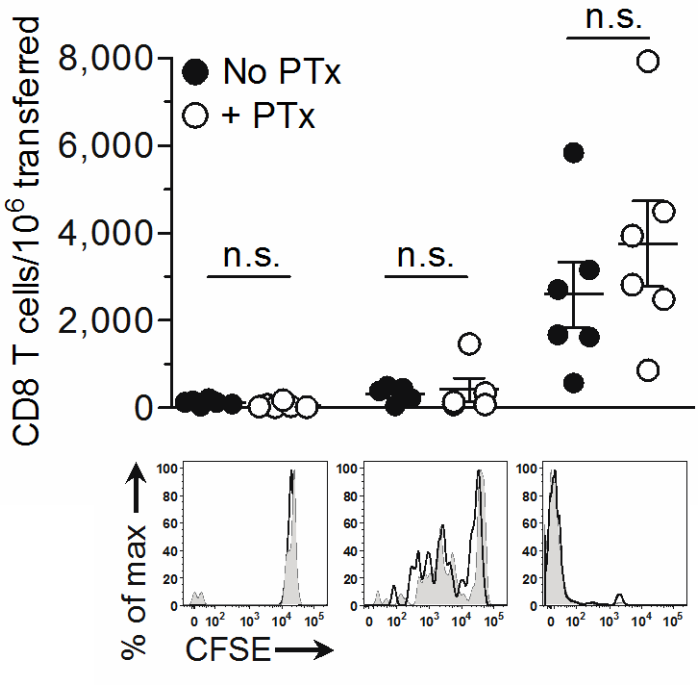

Figure 12. Gα_i-independent migration occurs in the absence of secondary lymphoid tissue.

PTx-treated and untreated T cells were co-transferred into recipients of BALB/c cardiac allografts 2 days after transplantation. Graph depicts enumeration of transferred memory $CD8^+$ T cells in the graft of splenectomized *aly*/*aly* recipients on day one, three and six after cell transfer. T cell proliferation for co-transferred cells treated with PTx (black outline) and untreated (grey) is shown in the CFSE histograms. Results are mean ± s.e.m.; n.s. = not significant.

Next, we extended our analysis of the migration of BALB/c primed allo-reactive T cells to vascularized organ transplants from memory T cells to effector T cells. The migration of $CD8^+$ effector T cells was examined utilizing the same experimental methods as previously detailed for memory T cells, except that grafts were removed at three and six days after cell transfer. Similar to results for memory T cells, $CD8^+$ effector T cells migrated to the grafts independent of Gα_i signaling (Figure 15).

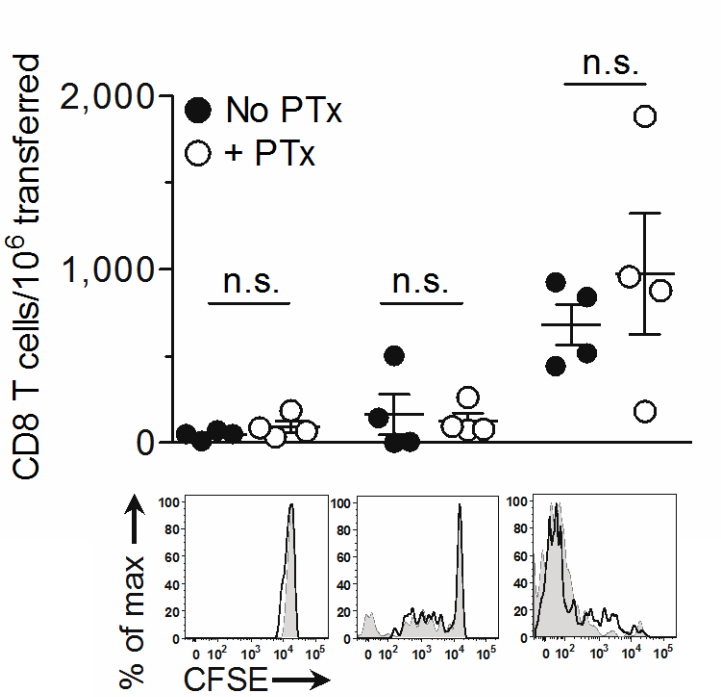

Figure 13. Acute graft inflammation is not required for Gα_i-independent T cell migration.

PTx-treated and untreated T cells were co-transferred into recipients of BALB/c cardiac allografts 50 days after transplantation. Graph depicts enumeration of transferred memory $CD8^+$ T cells in the graft of splenectomized *aly*/*aly* recipients on day one, three and six after cell transfer. T cell proliferation for co-transferred cells treated with PTx (black outline) and untreated (grey) is shown in the CFSE histograms. Results are mean ± s.e.m.; n.s. = not significant.

In contrast to our experimental findings for alloreactive BALB/c primed memory and effector T cells, neither naïve ($CD44^{low}$) (Figure 16) nor pre-existing (natural) memory (Figure 17) T cells transferred from non-immunized mice could be detected in significant numbers in the grafts.

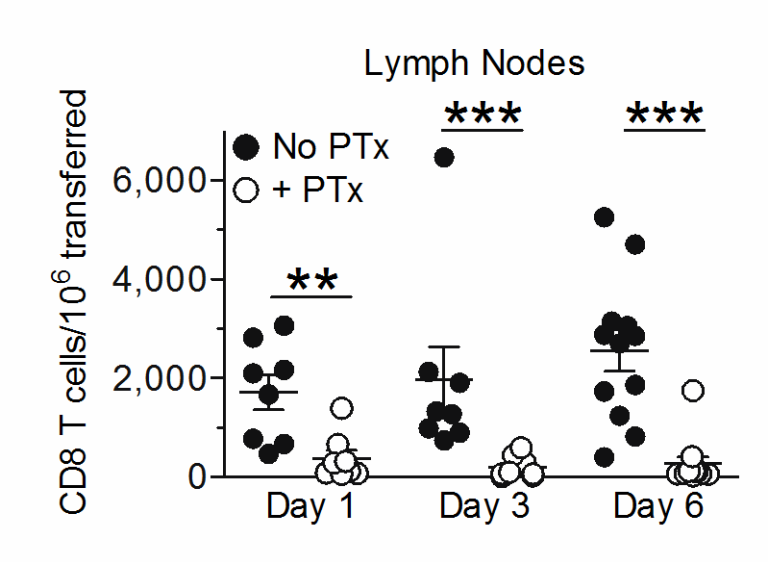

Figure 14. PTx treatment of transferred CD8 T cells blocks their migration to lymph nodes.

Graph depicts enumeration of co-transferred PTx treated (white) and untreated (black) $CD8^+$ memory T cells in the lymph nodes on day one, three and six after cell transfer. Results are mean ± s.e.m.; n.s. = not significant; *p<0.05, **p<0.01, ***p<0.001.

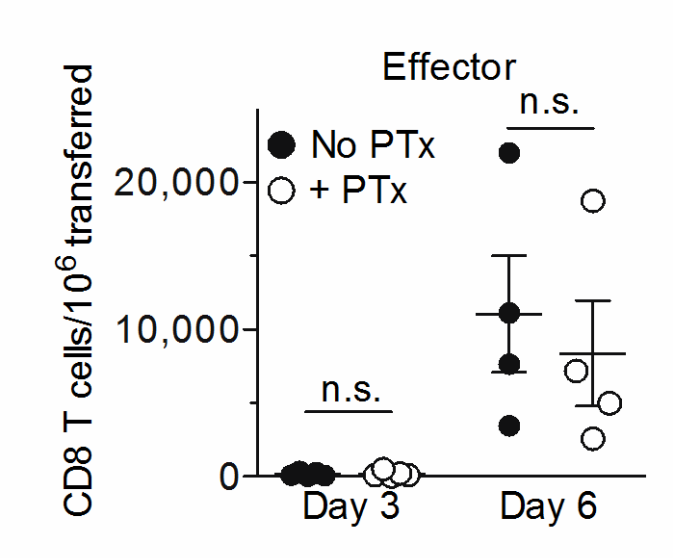

Figure 15. $G\alpha_i$-independent migration of effector T cells to heart allografts

PTx-treated and untreated T cells were co-transferred into recipients of BALB/c cardiac allografts 2 days after transplantation. Graph depicts enumeration of transferred effector $CD8^+$ T cells in the graft on day three and six after cell transfer. Results are mean ± s.e.m.; n.s. = not significant.

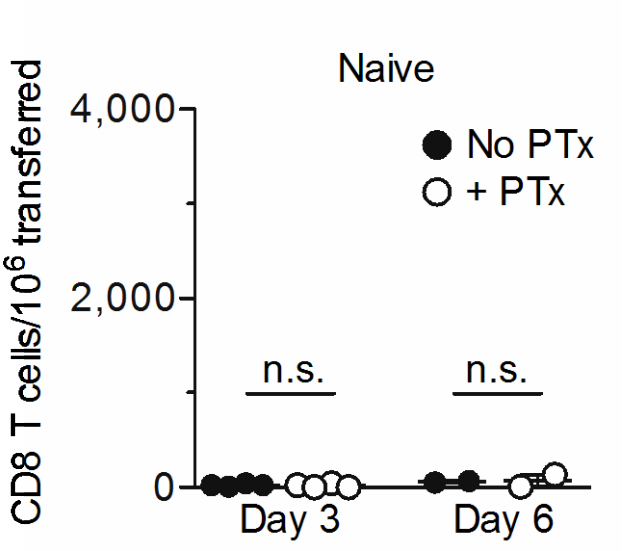

Figure 16. Transferred naïve T cells do not migrate of to heart allografts.

PTx-treated and untreated naïve T cells were co-transferred into recipients of BALB/c cardiac allografts 2 days after transplantation. Graph depicts enumeration of transferred naive $CD8^+$ T cells in the graft on day three and six after cell transfer. Results are mean ± s.e.m.; n.s. = not significant.

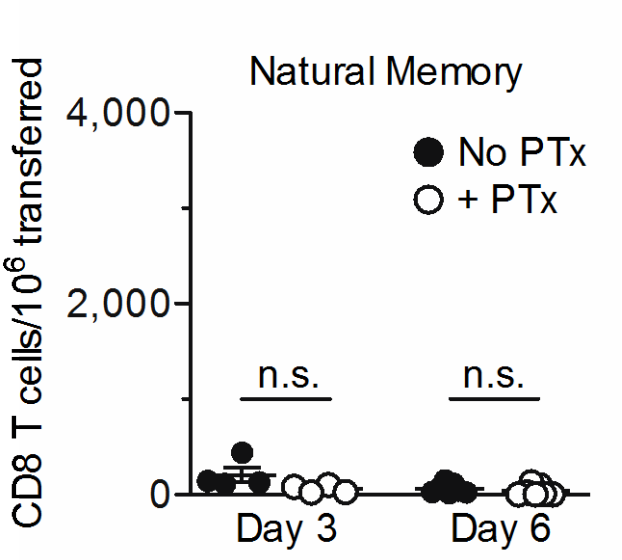

Figure 17. Transferred natural memory T cells do not migrate of to heart allografts.

PTx-treated and untreated natural memory T cells were co-transferred into recipients of BALB/c cardiac allografts 2 days after transplantation. Graph depicts enumeration of transferred natural memory $CD8^+$ T cells in the graft on day three and six after cell transfer. Results are mean ± s.e.m.; n.s. = not

Using splenectomized *aly/aly* recipients in which allograft rejection is dependent on the transfer of effector or memory T cells [2, 3], we observed that PTx-treated memory T cells cause acute rejection of heart allografts albeit with a short but not significant delay compared to their untreated counterparts (Figure 18).

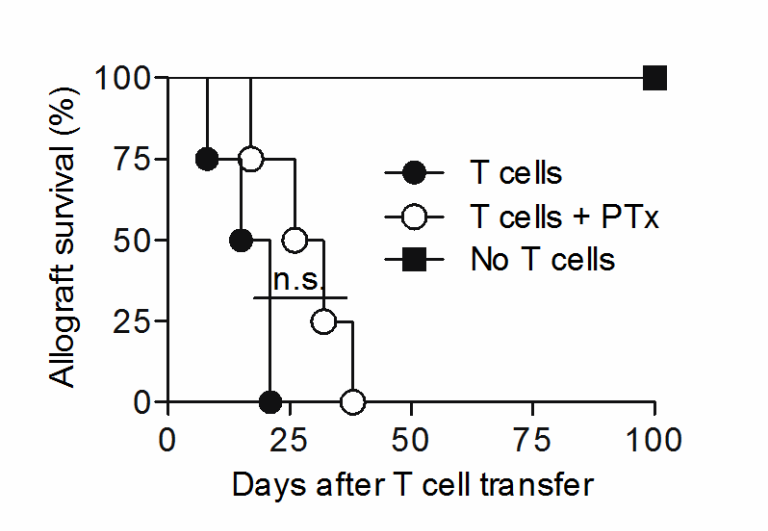

Figure 18. Memory T cell mediated rejection of heart allografts occurs independent of Gα_i.

PTx-treated or untreated memory T cells were transferred into recipients of BALB/c cardiac allografts 2 days after transplantation. Graph depicts heart allograft survival in splenectomized *aly*/*aly* recipients that received either PTx-treated or untreated memory T cells. Results are mean ± s.e.m.; n.s. = not significant; *p<0.05, **p<0.01, ***p<0.001.

Taken together, these results indicate that, contrary to the prevailing view, Gα_i-dependent chemokine receptor signaling is not necessary for the migration of effector and memory T cells to vascularized organ transplants.

3.2 COGNATE ANTIGEN DIRECTS THE MIGRATION OF CD8$^+$ EFFECTOR T CELLS TO VASCULARIZED ALLOGRAFTS

An alternative mechanism that could govern effector or memory T cell migration and accumulation in the tissues is interaction of the T cell receptor (TCR) with cognate antigen presented by the endothelium or tissue antigen antigen-presenting cells (APC) [58-62]. Similar to chemokine receptors, the TCR triggers inside-out signaling that changes the conformation of integrins (namely, LFA-1 and VLA-4) from a low to a high affinity ligand binding state [63, 65, 66]. Unlike chemokine receptors, however, inside-out signaling via the TCR is independent of $G\alpha_i$ [63, 64]. Since we observed that blocking $G\alpha_i$ does not impede the migration of effector or memory T cells to the grafted tissue, we asked whether TCR engagement by cognate antigen drives the migration process.

To test this possibility, we transplanted B6-OVA transgenic hearts, which express the non-self antigen ovalbumin (OVA), or syngeneic B6 hearts, which do not express OVA, into B6 recipients and then co-transferred PTx-treated and untreated TCR-transgenic OT-I or P14 CD8$^+$ effector T cells. All T cell transfers were performed two days after heart transplantation. Since OVA is recognized by the OT-I but not the P14 TCR (Figure 19), this model allowed us to dissect the requirements for the migration of antigen-specific (OT-I) and non-specific (P14) T cells.

On day 3 after cell transfer, both PTx-treated and untreated OT-I effector cells were present in B6-OVA grafts in comparable numbers (Figure 20) and had proliferated equally (Figure 21). In contrast, OT-I cells did not migrate to wild-type B6 grafts that lack OVA, and neither PTx-treated nor untreated P14 effector cells, which do not recognize OVA, migrated to B6-OVA

grafts (Figure 20). PTx-treated OT-I cells did not home to lymph nodes in these experiments (Figure 22), indicating that $G\alpha_i$ was adequately blocked. Moreover, PTx-treated OT-I effector T

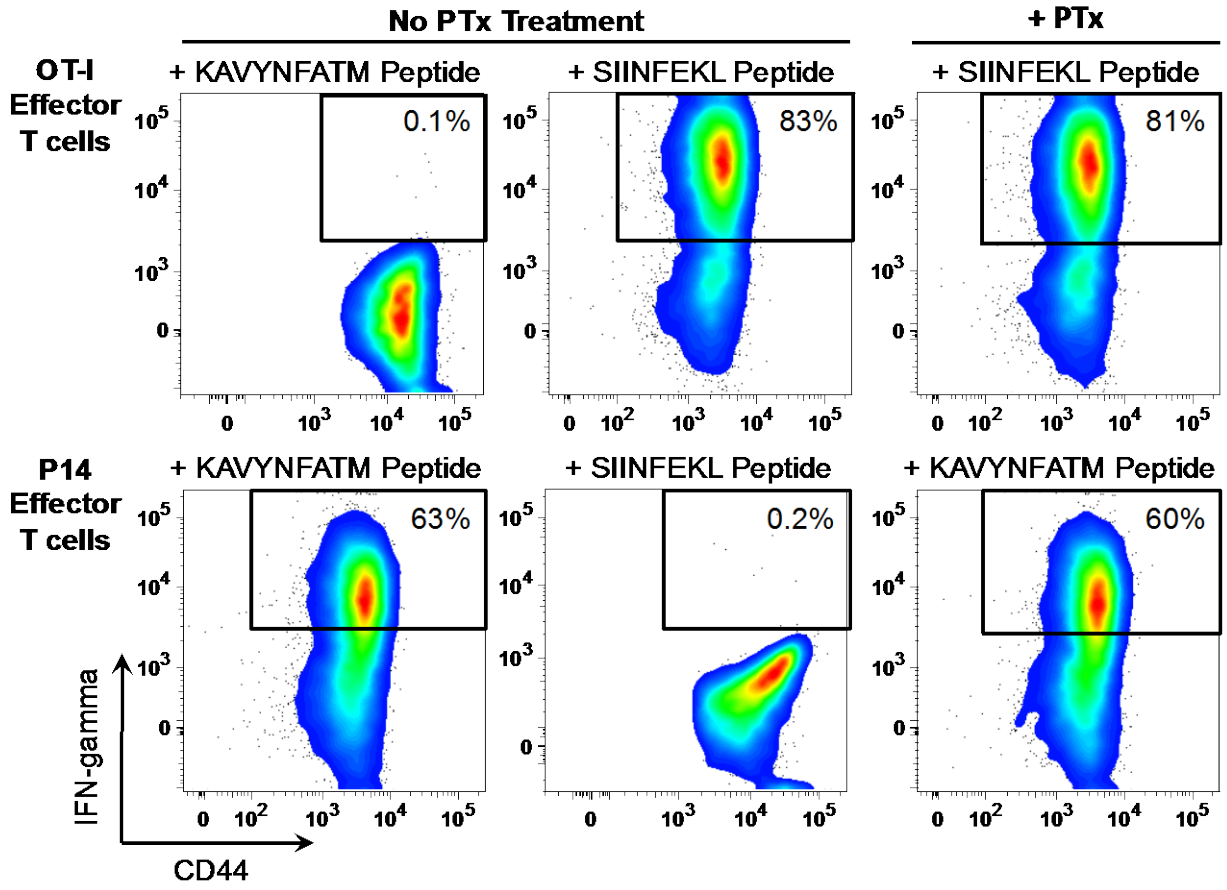

Figure 19. Monoclonal effector T cells react specifically to their cognate Ag with or without PTx.

Monoclonal OT-I (specific to the SIINFEKL peptide of the OVA antigen) and P14 (specific to the KAVYNFATM peptide located in the GP33 epitope of the LCMV virus) $CD8^+$ effector T cells were generated in vivo by co-transfer of naïve T cells with their respective peptide-pulsed bone marrow derived dendritic cells. OT-I and P14 $CD8^+$ effector T cells were then either treated with PTx or not and incubated overnight with either SIINFEKL or KAVYNFATM peptide-pulsed dendritic cells. Intracellular cytokine staining and subsequent flow cytometry analysis depicts the percentage of OT-I and P14 $CD8^+CD44^+$ effector T cells expressing interferon gamma. Flow plots are from one representative experiment. Three independent experiments were performed with OT-I effector T cells. Two independent experiments were performed with the P14 effector T cells.

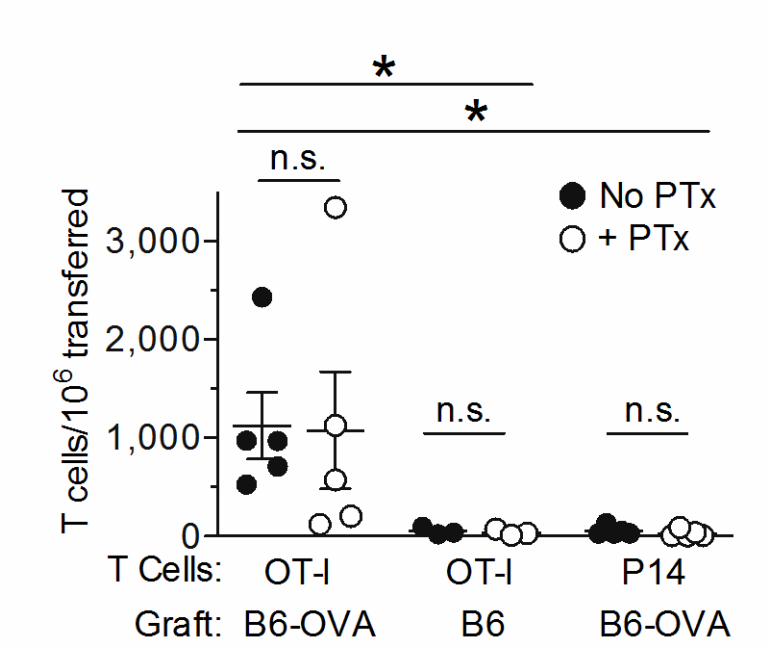

Figure 20. Cognate antigen directs the migration of effector T cells to heart grafts.

PTx-treated and untreated OT-I or P14 effector T cells were co-transferred into recipients 2 days after transplantation of heart grafts which either express (B6-OVA) or do not express (B6) the cognate antigen for OT-I T cells. Transferred cells were enumerated in the grafts 3 days after transfer. Results are mean ± s.e.m.; n.s. = not significant; *p<0.05, **p<0.01, ***p<0.001.

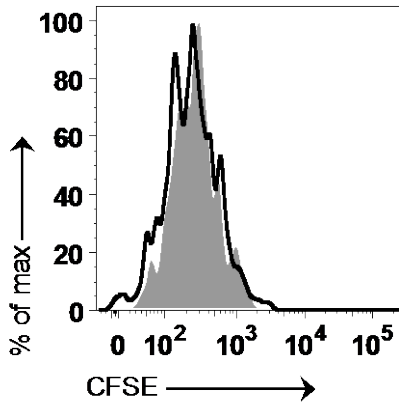

Figure 21. OT-I effector T cells proliferate in B6-OVA grafts on day 3 with or without PTx.

PTx-treated and untreated OT-I effector T cells were co-transferred into recipients 2 days after transplantation of heart grafts that express (B6-OVA) the cognate antigen for OT-I T cells. T cell proliferation for co-transferred cells treated with PTx (black outline) and untreated (grey) is shown in the CFSE histograms.

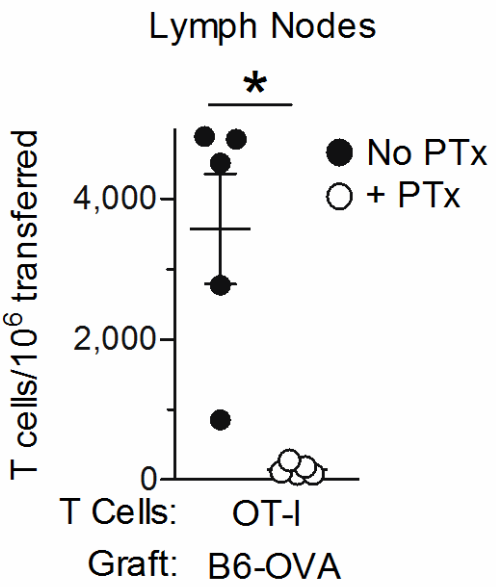

Figure 22. PTx treatment of transferred CD8$^+$ T cells blocks their migration to lymph nodes.

Graph depicts enumeration of co-transferred PTx treated (white) and untreated (black) OT-I CD8$^+$ effector T cells in the recipient's lymph nodes on day three after cell transfer. Results are mean ± s.e.m.; n.s. = not significant; *p<0.05, **p<0.01, ***p<0.001.

cells did not migrate in response to a chemokine gradient *in vitro*, either before or after restimulation with antigenic peptide, further confirming irreversible inhibition of $G\alpha_i$ function in these cells (Figure 23).

Anti-VLA4 antibodies blocked the migration of PTx-treated OT-I effector cells to the graft (Figure 24), indicating that integrin activation, occurring via a $G\alpha_i$-independent pathway, was still required for effector T cell migration. These findings indicate that cognate antigen recognition is necessary for integrin-dependent migration of antigen-specific effector T cells to the graft while $G\alpha_i$ signaling is not required.

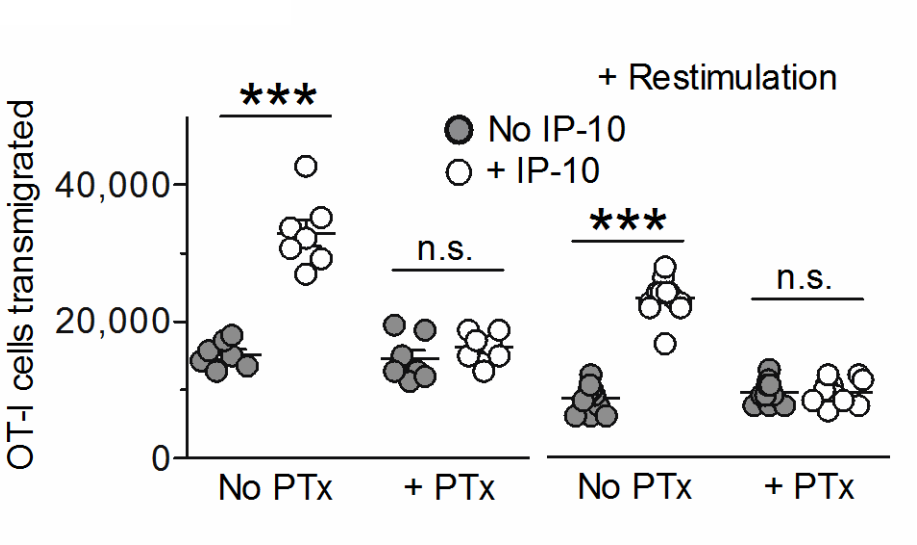

Figure 23. PTx treatment blocks the *in-vitro* migration of re-stimulated OT-I effector T cells.

In vitro migration of PTx-treated and untreated OT-I effector T cells in response to IP-10 before and 6 hours after re-stimulation with cognate antigen. Results are mean ± s.e.m.; n.s. = not significant; *p<0.05, **p<0.01, ***p<0.001.

To study the requirements for the migration of non-specific (bystander) T cells, we co-transferred P14 and OT-I effector cells with or without PTx treatment to recipients of B6-OVA grafts. P14 cells migrated to the graft only when antigen-specific OT-I cells were present and only P14 migration was inhibited when both cell populations were treated with PTx (Figure 25). In contrast, the migration of OT-I cells to the graft was independent of both P14 cells and $G\alpha_i$ signaling (Figure 26). Therefore, migration of antigen non-specific (bystander) T cells to the graft is dependent on both antigen-specific effector T cells and $G\alpha_i$.

To investigate the roles of cognate antigen and $G\alpha_i$ in the transmigration of effector T cells across the graft endothelium, we performed real-time, two-photon intravital imaging of mouse kidney transplants, a procedure we had established in our laboratory [69]. Unlike the

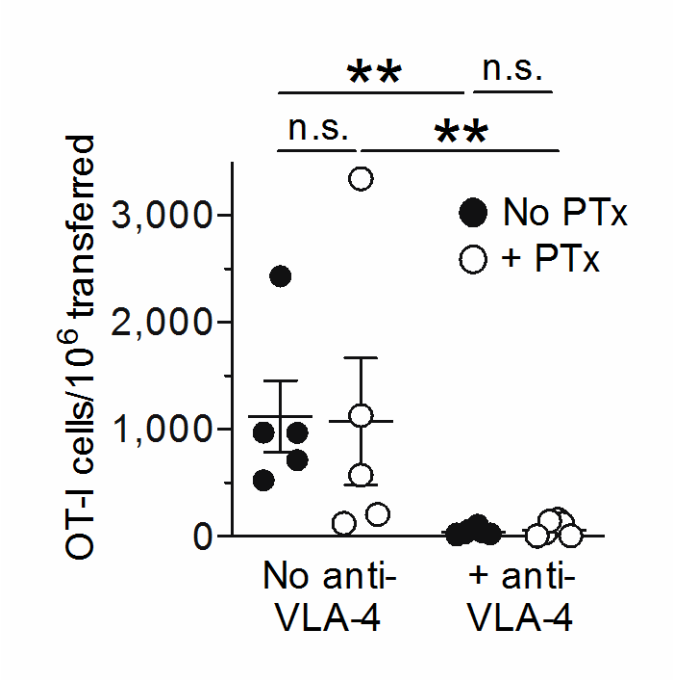

Figure 24. VLA-4 is required for the migration of OT-I effector T cells to B6-OVA heart grafts.

PTx-treated and untreated OT-I effector T cells were co-transferred into recipients 2 days after transplantation of B6-OVA heart grafts which express the cognate antigen for OT-I T cells. Transplant recipients were either injected (i.p.) with anti-VLA-4 antibody or not. Transferred OT-I cells were enumerated in the grafts 3 days after co-transfer. Control group (No anti-VLA-4) was taken from the first experimental group in Figure 20. Results are mean ± s.e.m.; n.s. = not significant; *p<0.05, **p<0.01, ***p<0.001.

flow cytometry approach utilized in Figure 20, intravital microscopy permitted the direct visualization and enumeration of T cells early after transfer, prior to their proliferation in the graft (Figure 27). It also allowed us to determine whether they had firmly adhered to the capillary wall or transmigrated and to calculate their motility parameters.

PTx-treated and untreated antigen-specific (OT-I) or bystander (P14) effectors were transferred into B6 recipients of either B6-OVA or B6 kidney grafts two days after transplantation and the grafts were imaged 24 hours later. OT-1 and P14 cells present in 30

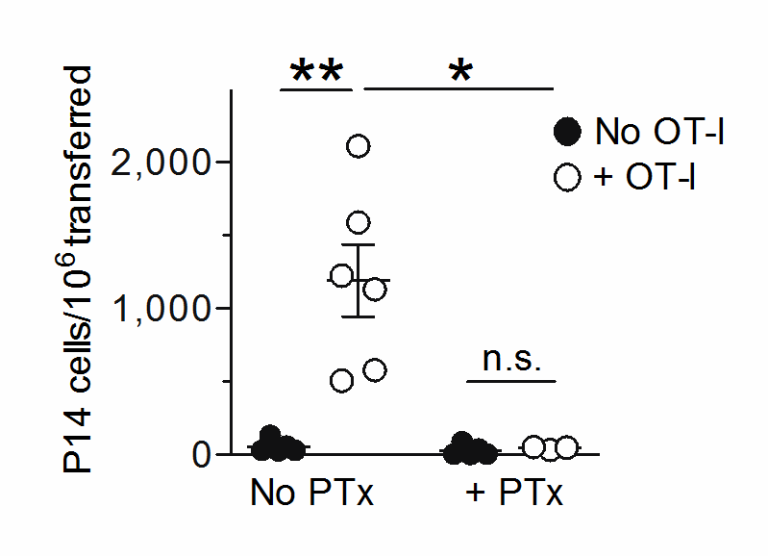

Figure 25. Migration of non-specific effector T cells requires antigen specific cells and Gα_i signaling.

PTx-treated and untreated P14 effector T cells were transferred with (white) or without (black) OT-I cells into recipients 2 days after transplantation of B6-OVA heart grafts expressing the cognate antigen for OT-I T cells. Transferred P14 cells were enumerated in the grafts 3 days after transfer. Control group (No OT-I) was taken from the third experimental group in Figure 20. Results are mean ± s.e.m.; n.s. = not significant; *p<0.05, **p<0.01, ***p<0.001.

second-long z-stacks (image volumes) were enumerated at multiple representative time points and in multiple tissue locations. As shown in Figure 28 (Supplemental Movies 1 & 2), OT-I cells migrated to B6-OVA, but not control B6 kidney grafts and their migration was not inhibited by PTx. In contrast, the migration of non-specific (P14) T cells to B6-OVA grafts was considerably less than that of OT-I cells (15 ± 4.3 *vs* 101 ± 3 cells per image volume, mean ± s.e.m., p<0.001) and was inhibited by PTx (Figure 28, Supplemental Movie 3). These results confirm the primary role cognate antigen has in effector T cell migration to organ transplants. Similar to heart graft data shown in Figure 25, substantial migration of antigen-non-specific (P14) T cells to kidney

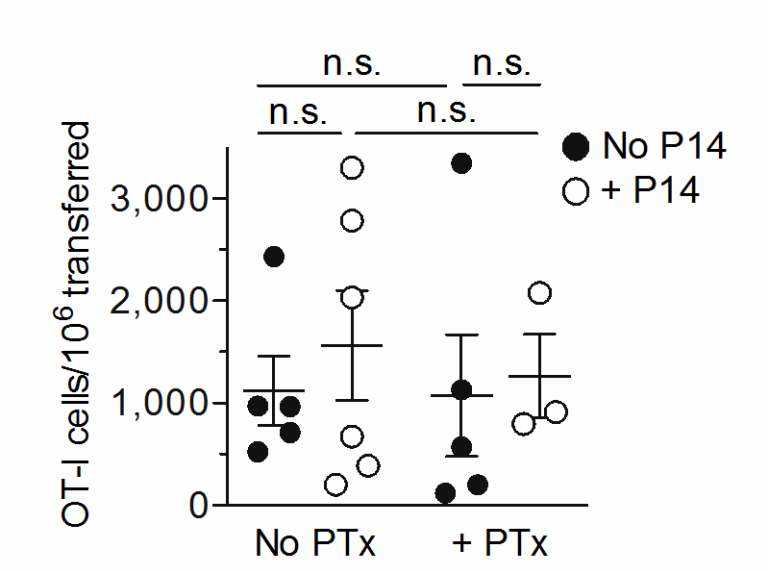

Figure 26. Migration of Ag specific T cells does not require "bystander" T cells or Gα_i signaling.

PTx-treated and untreated OT-I effector T cells were transferred with (white) or without (black) P14 cells into recipients 2 days after transplantation of B6-OVA heart grafts expressing the cognate antigen for OT-I T cells. Transferred OT-I cells were enumerated in the grafts 3 days after transfer. Control groups (No P14) are taken from the first experimental group in Figure 20. Results are mean ± s.e.m.; n.s. = not significant; *p<0.05, **p<0.01, ***p<0.001.

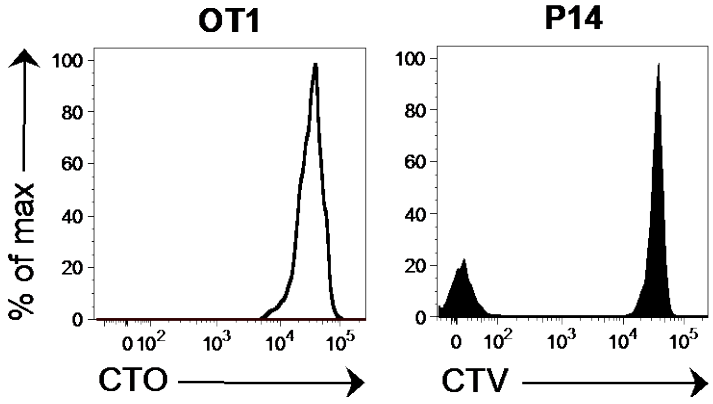

Figure 27. OT-I and P14 effector T cells do not proliferate in OVA grafts 24 hours after transfer.

Cell tracker orange (CTO) stained OT-I and cell trace violet stained (CTV) P14 effector T cells were co-transferred into B6-OVA kidney graft recipients 2 days after transplantation. Grafts were harvested and analyzed by flow cytometry 24 hours after cell transfer. T cell proliferation for co-transferred cells treated is shown in the histograms.

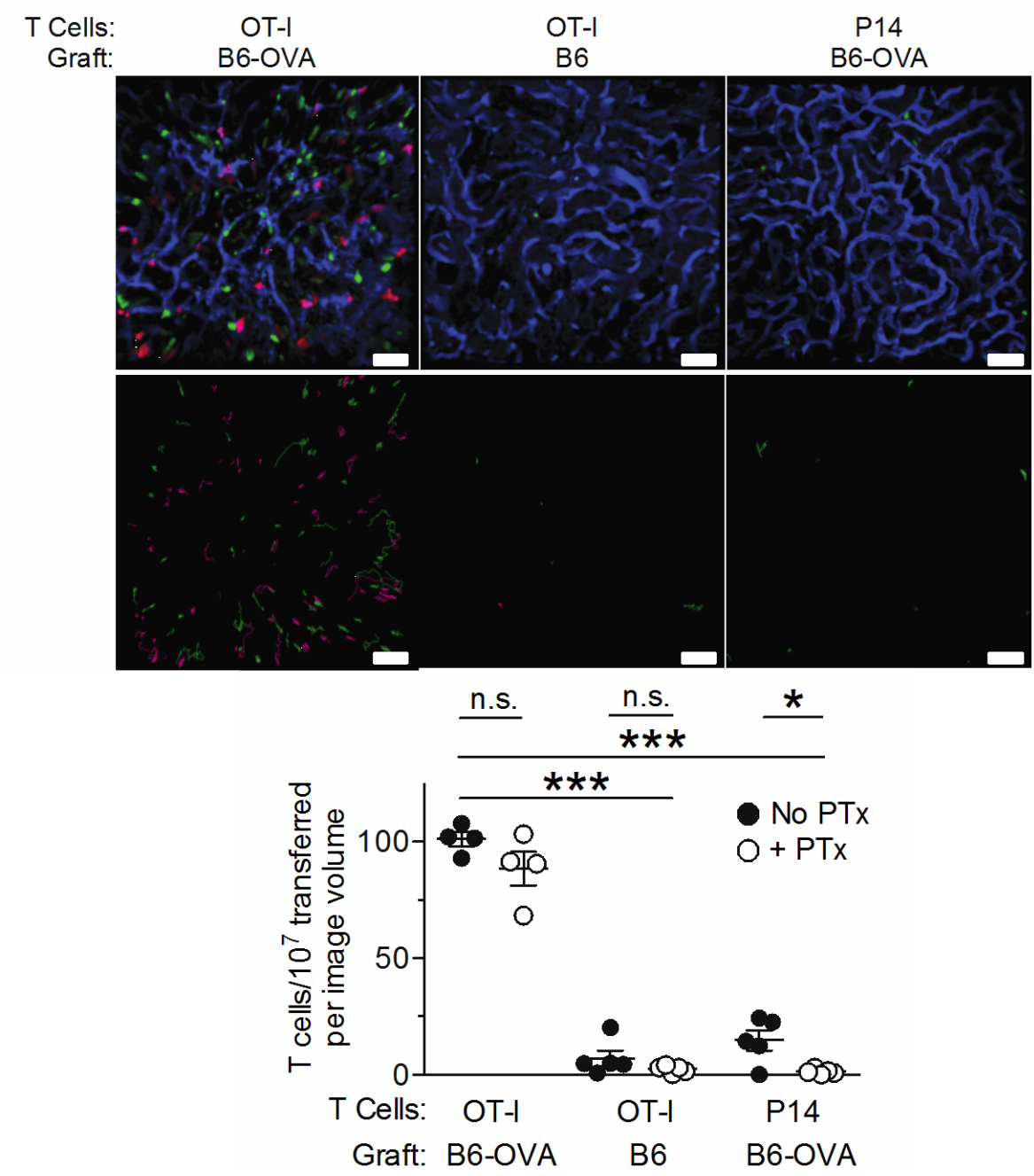

Figure 28. Cognate antigen directs the migration of effector T cells to kidney grafts.

OT-I and P14 effector T cells were transferred into kidney graft recipients 2 days after transplantation. Grafts were imaged 24 hours after cell transfer. Z-stacks (0.45 x 0.45 x 0.03 mm) were obtained at 30 second intervals. Visualization (image panels) and enumeration (graph) of PTx-treated and untreated OT-I and P14 cells arrested in B6-OVA or B6 kidney grafts (n = 4-5 movies/group, two independent experiments). Top image panels are volume-rendered representative time point images showing arrested PTx-treated (red) and untreated (green) cells in each of the experimental groups. Blood vessels

are labeled in blue. Bottom panels are time projections of 30 min depicting PTx-treated (red) and untreated (green) cell tracks. Scale bars, 50 μm. Results are mean ± s.e.m.; n.s. = not significant; *p<0.05, **p<0.01,

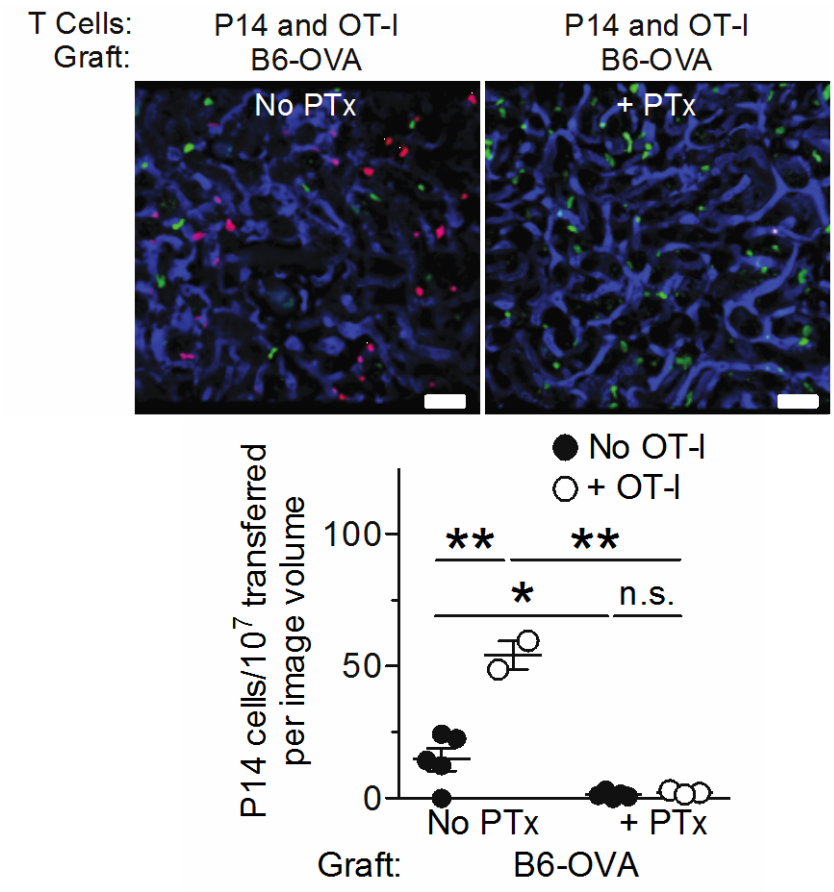

Figure 29. Migration of non-specific T cells requires Ag specific OT-I cells and $G\alpha_i$ signaling.

OT-I and P14 effector T cells were transferred into kidney graft recipients 2 days after transplantation. Grafts were imaged 24 hours after cell transfer. Z-stacks (0.45 x 0.45 x 0.03 mm) were obtained at 30 second intervals. Image panels are volume-rendered representative time point images of B6-OVA grafts after co-transfer of P14 (red) and OT-I (green) cells that were either treated with PTx or not. Blood vessels are labeled in blue. Graph is enumeration of P14 cells arrested in B6-OVA kidney grafts in the presence or absence of OT-I cells and PTx (n = 2-5 movies/group, two independent experiments). Control groups (No OT-I) are taken from the third experimental group in Figure 28. Scale bars, 50 μm. Results are mean ± s.e.m.; n.s. = not significant; *p<0.05, **p<0.01, ***p<0.001.

grafts was observed only when co-transferred with antigen-specific (OT-I) cells and was completely inhibited by PTx (Figure 29).

To determine the location of T cells in the graft, we tracked OT-I and P14 cells for >2 minutes and ascertained whether they were arrested inside the capillaries or had transmigrated to the extra-capillary space. We found that approximately half of the OT-I cells were firmly adhered inside the capillary lumina while a similar proportion had transmigrated (Figure 30 and Figure 31). Pre-treatment with PTx did not reduce the number of either firmly adhered or transmigrated OT-I cells but completely inhibited the adhesion and transmigration of non-specific T cells (P14) (Figure 30 and Figure 31). A PTx-treated OT-I cell tracked transmigrating across the capillary wall of a B6-OVA graft is shown in Figure 32.

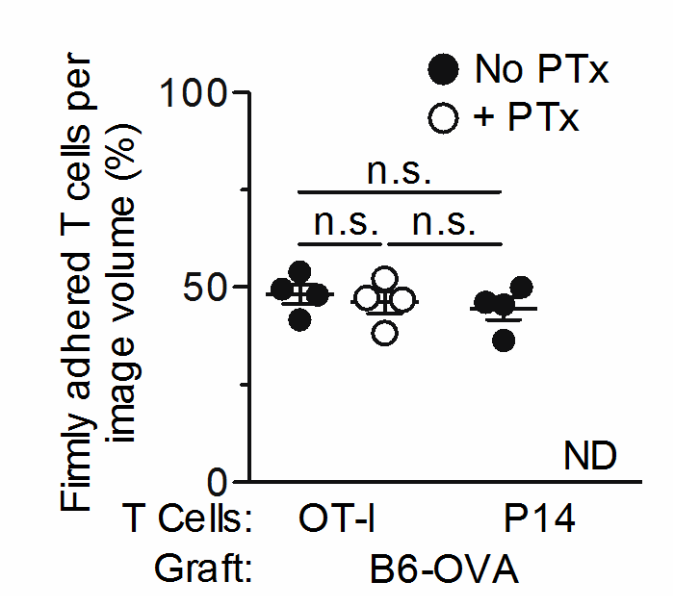

Figure 30. Ag specific effector T cells firmly adhere to the graft vascular lumen independent of $G\alpha_i$.

Percent of OT-I and P14 cells, tracked in the experiment shown in Figure 28 that had firmly adhered to the capillary wall of B6-OVA kidney grafts. Results are mean ± s.e.m.; n.s. = not significant; *p<0.05, **p<0.01, ***p<0.001.

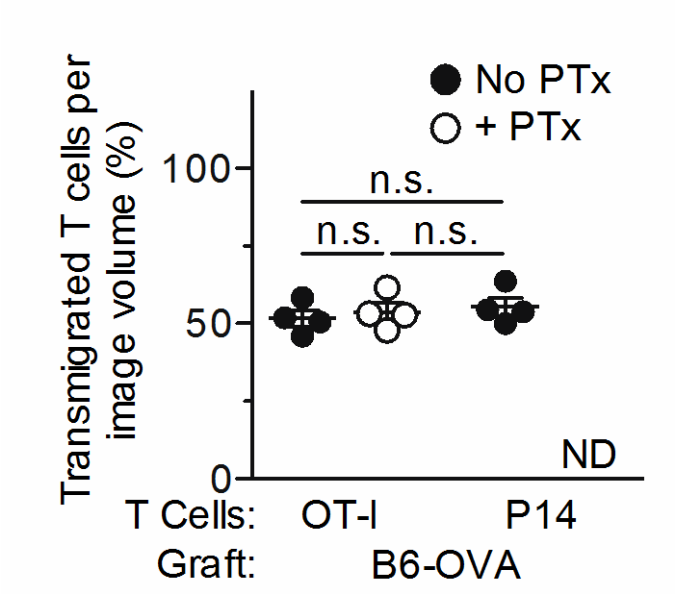

Figure 31. Ag specific effector T cells undergo transendothelial migration independent of $G\alpha_i$.

Percent of OT-I and P14 cells tracked in the experiment shown in Figure 28 that had transmigrated into the extra-capillary space of B6-OVA kidney grafts. Results are mean ± s.e.m.; n.s. = not significant; *p<0.05, **p<0.01, ***p<0.001.

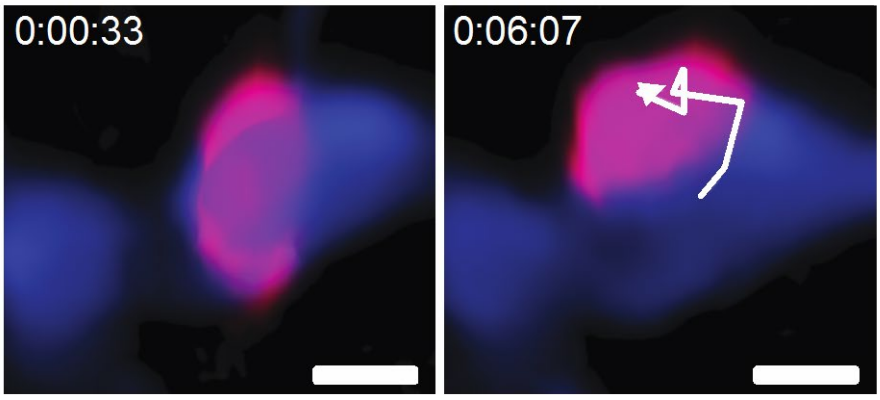

Figure 32. Images of a PTx-treated OT-I cell transendothelial migrating in an OVA kidney graft.

Time-lapse images showing the transendothelial migration of a PTx-treated OT-I cell (red) in a B6-OVA kidney graft. Cell was tracked in the experiment shown in Figure 28. Blood vessel is labeled in blue. Scale bars, 10 μm.

Motility analysis confirmed that the majority of PTx-treated and untreated OT-I cells and untreated P14 cells enumerated in Figure 28 had arrested in the graft, as judged by their low velocities, short displacements, and high arrest coefficients (Figure 33, Figure 34 and Figure 35) [86]. Significant differences in the motility of the three cell populations, however, were observed. Antigen-specific (OT-I cells) had lower velocities and higher arrest coefficients than non-specific P14 cells. Moreover, blocking $G\alpha_i$ in OT-I cells increased their velocity and reduced their arrest coefficient but they remained significantly less motile than P14 cells (Figure 33, Figure 34 and Figure 35).

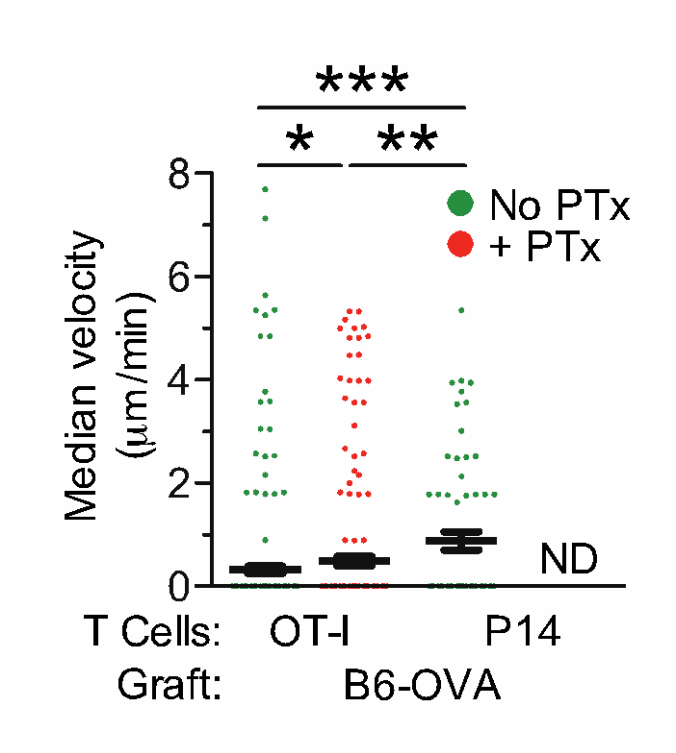

Figure 33. Ag specific cells have a lower velocity than bystander cells in grafts with cognate Ag.

Median velocity of PTx-treated (n = 223) or untreated (n = 265) OT-I cells and P14 cells without PTx treatment (n = 68) imaged in B6-OVA grafts. Cells were tracked in the experiments shown in Figure 28. Results are mean ± s.e.m.; n.s. = not significant; *p<0.05, **p<0.01, ***p<0.001.

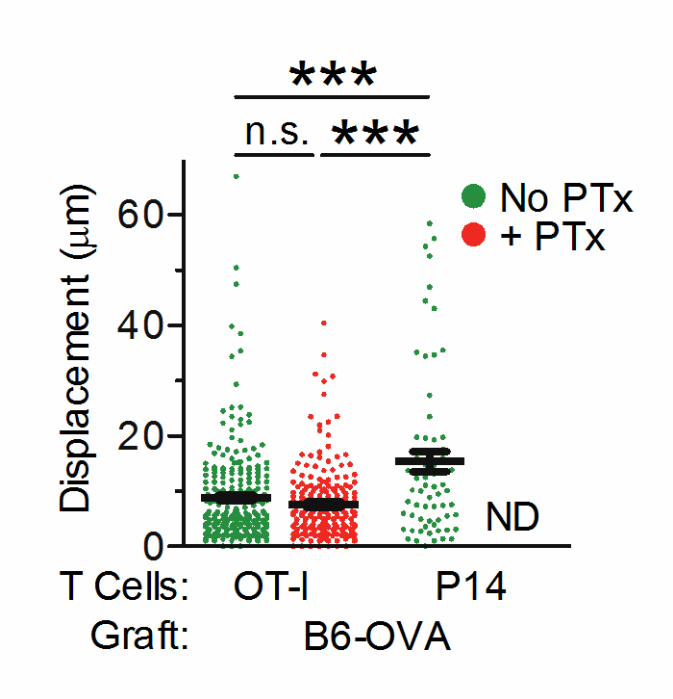

Figure 34. Ag specific cells have less displacement than bystander cells in grafts with cognate Ag.

Displacement of PTx-treated (n = 223) or untreated (n = 265) OT-I cells and P14 cells without PTx treatment (n = 68) imaged in B6-OVA grafts. Cells were tracked in the experiments shown in Figure 28. Results are mean ± s.e.m.; n.s. = not significant; *p<0.05, **p<0.01, ***p<0.001.

Together, these findings indicate that antigen-specific effector T cells firmly adhere to and transmigrate across the graft endothelium in an antigen-dependent, $G\alpha_i$-independent fashion. However, non-specific (bystander) effector T cells are dependent on the presence antigen-specific effector T cells and $G\alpha_i$ signaling to enter the graft tissue.

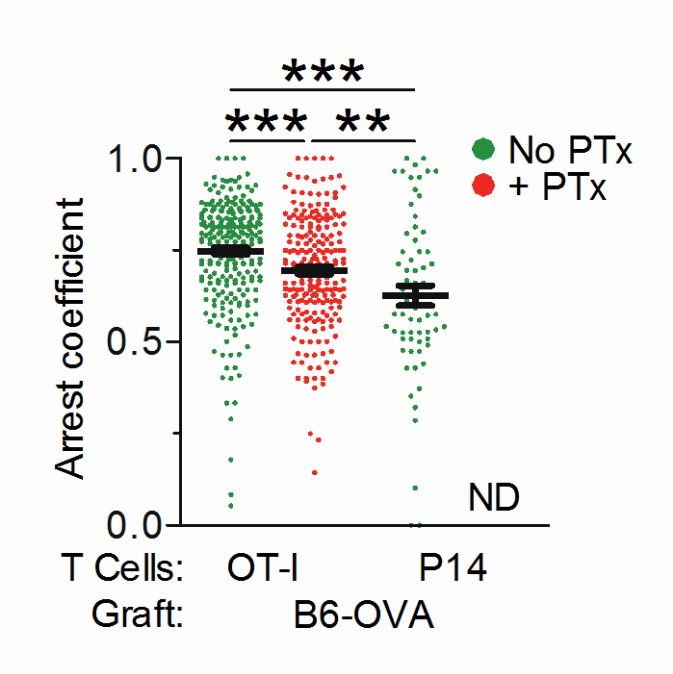

Figure 35. Ag specific cells are arrested more than bystander cells in grafts with cognate Ag.

Arrest coefficient of PTx-treated (n = 223) or untreated (n = 265) OT-I cells and P14 cells without PTx treatment (n = 68) imaged in B6-OVA grafts. Cells were tracked in the experiments shown in Figure 28. Results are mean ± s.e.m.; n.s. = not significant; *p<0.05, **p<0.01, ***p<0.001.

3.3 PRESENTATION OF COGNATE ANTIGEN BY EITHER GRAFT ENDOTHELIUM OR BONE MARROW DERIVED APC IS SUFFICIENT FOR THE TRANSMIGRATION OF EFFECTOR T CELLS

We next sought to determine which graft cell is responsible for presenting antigen to migrating T cells. Although it is suspected that antigen presentation in the vascular lumen is an exclusive function of endothelial cells [87], bone marrow derived APC such as dendritic cells are known to extend cellular processes across endothelial and epithelial barriers in several tissues [88-90]. We therefore analyzed by two-photon microscopy the migration of effector OT-I cells to B6-OVA kidney grafts that lack the MHC class I molecule H-2K^b (which is required for presenting cognate OVA peptide to OT-I cells) on the endothelium, bone marrow derived APC, or both.

As shown in Figure 36, Figure 37 and Figure 38 (Supplemental Movies 4-6), H-2K^b expression on either graft APC or endothelium was sufficient for the firm adhesion and transmigration of OT-1 effectors. In either case, however, migration was slightly less than that observed if H-2K^b was present on both cell types (compared to data in Figure 28, $p < 0.05$), while total absence of H-2K^b in the graft reduced migration to minimal levels (Figure 36). Motility analysis revealed that antigen presentation by bone marrow derived APC caused a greater degree of effector T cell arrest than endothelial cells (Figure 39, Figure 40, and Figure 41). This conclusion was true for total effector T cells in the graft as well as those arrested in the capillary lumen (Figure 39, Figure 40, and Figure 41).

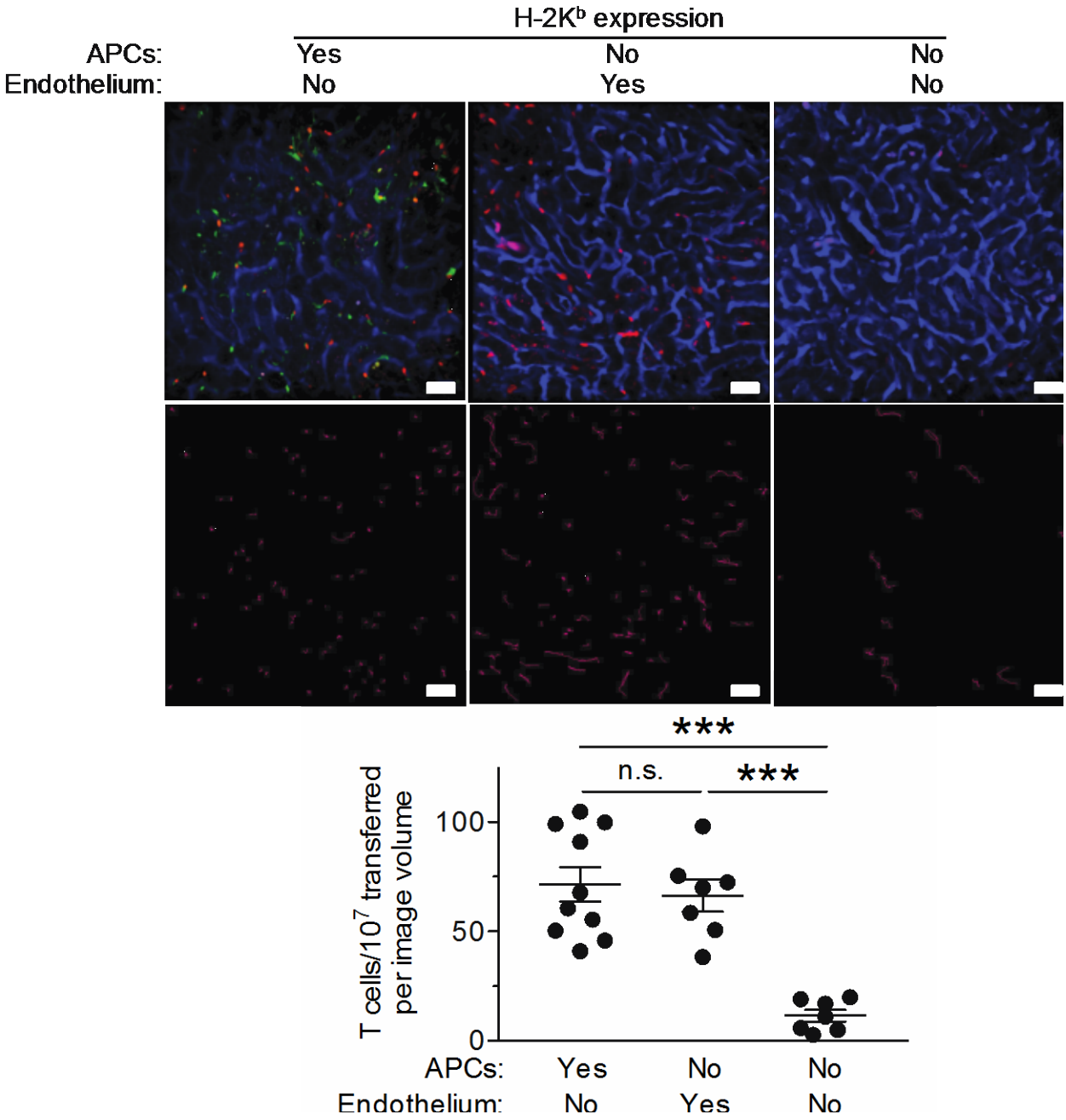

Figure 36. Effector T cell migration is promoted by endothelial or APC presentation of cognate Ag.

OT-I effector T cells were transferred into kidney graft recipients 2 days after transplantation. Grafts were imaged by multiphoton intravital microscopy 24 hours after cell transfer. Visualization (image panels) and enumeration (graph) of OT-I cells arrested in B6-OVA kidney grafts that lack H-2K^b expression on the endothelium (WT to H-2k$^{b-/-}$ chimeric graft to WT recipient), APC (H-2k$^{b-/-}$ to WT chimeric graft to H-2k$^{b-/-}$ recipient), or both (H-2k$^{b-/-}$ graft to H-2k$^{b-/-}$ recipient) (n = 7-10 movies/group, 2 – 3 independent experiments). Top panels are volume-rendered representative time point images showing arrested OT-I cells (red). Green cells in top left panel are

CD11c-YFP^{+} dendritic cells. Blood vessels are labeled in blue. Bottom panels are time projections depicting OT-I cells (red) tracked over approximately 30 min. Scale bars, 50 μm. Results are mean ± s.e.m.; n.s. = not significant; *p<0.05, **p<0.01, ***p<0.001.

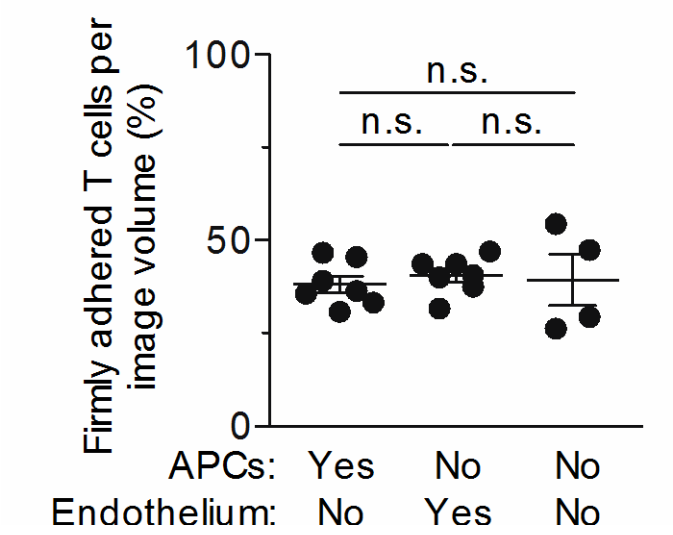

Figure 37. Effector T cells firmly adhere irrespective of endothelial or APC Ag presentation.

OT-I effector T cells were transferred into B6-OVA kidney graft recipients 2 days after transplantation. B6-OVA kidney grafts that lack H-2K^{b} expression on the endothelium, APC or both were imaged by multiphoton intravital microscopy 24 hours after cell transfer. Percent of OT-I cells tracked in the experiments shown in Figure 36 that had firmly adhered to the capillary wall of the kidney grafts. Results are mean ± s.e.m.; n.s. = not significant; *p<0.05, **p<0.01, ***p<0.001.

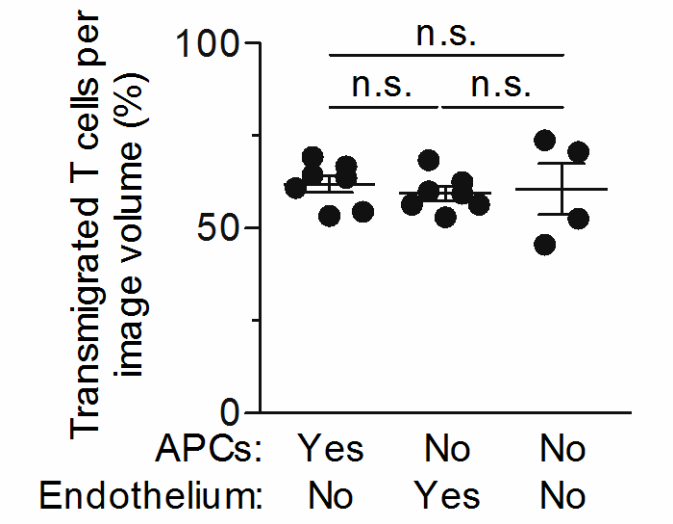

Figure 38. Effector T cells arrested in the graft transmigrate irrespective of Ag presentation.

OT-I effector T cells were transferred into B6-OVA kidney graft recipients 2 days after transplantation. B6-OVA kidney grafts that lack H-2K^b expression on the endothelium, APC or both were imaged by multiphoton intravital microscopy 24 hours after cell transfer. Percent of OT-I cells tracked in the experiments shown in Figure 36 that had transmigrated into the extra-capillary space of the kidney grafts. Results are mean ± s.e.m.; n.s. = not significant; *p<0.05, **p<0.01, ***p<0.001.

Imaging of OT-1 effectors in B6-OVA kidneys in which bone marrow derived dendritic cells (DC) are genetically labeled with YFP confirmed that the majority of arrested T cells, irrespective of location, make stable contacts with graft DC (Figure 42). An example of an OT-I cell arresting in the capillary lumen after contact with a DC is shown graphically (instantaneous velocity *vs* time) and in time lapse images in Figure 43 (Supplemental Movie 7). Furthermore, OT-I cells maintained contact with graft DC throughout the transmigration process (example shown in Figure 44, Supplemental Movie 8). These findings establish bone marrow derived graft APC as an alternative but remarkably robust pathway by which effector T cells firmly adhere to and transmigrate across the capillary wall.

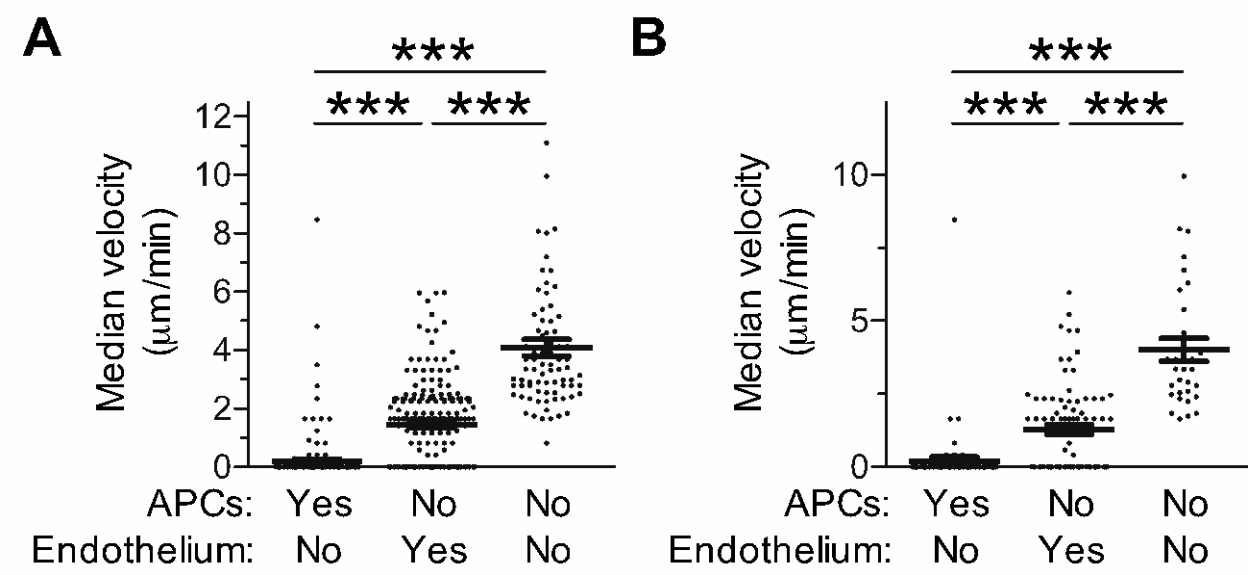

Figure 39. Graft endothelial or APC Ag presentation lowers the velocity of effector T cells.

OT-I effector T cells were transferred into B6-OVA kidney graft recipients 2 days after transplantation. Grafts were imaged by multiphoton intravital microscopy 24 hours after cell transfer and cell tracks are shown in Figure 36. (**A**) Median velocity of all OT-I cells tracked in B6-OVA kidney grafts that lack H-2K^b expression on the endothelium (n = 168), APC (n = 206) or both (n = 77). (**B**) Median velocity of tracked OT-I cells that remained inside the vascular lumen without transmigrating in B6-OVA kidney grafts that lack H-2K^b expression on the endothelium (n = 65), APC (n = 81), or both (n = 31). Results are mean ± s.e.m.; n.s. = not significant; *p<0.05, **p<0.01, ***p<0.001.

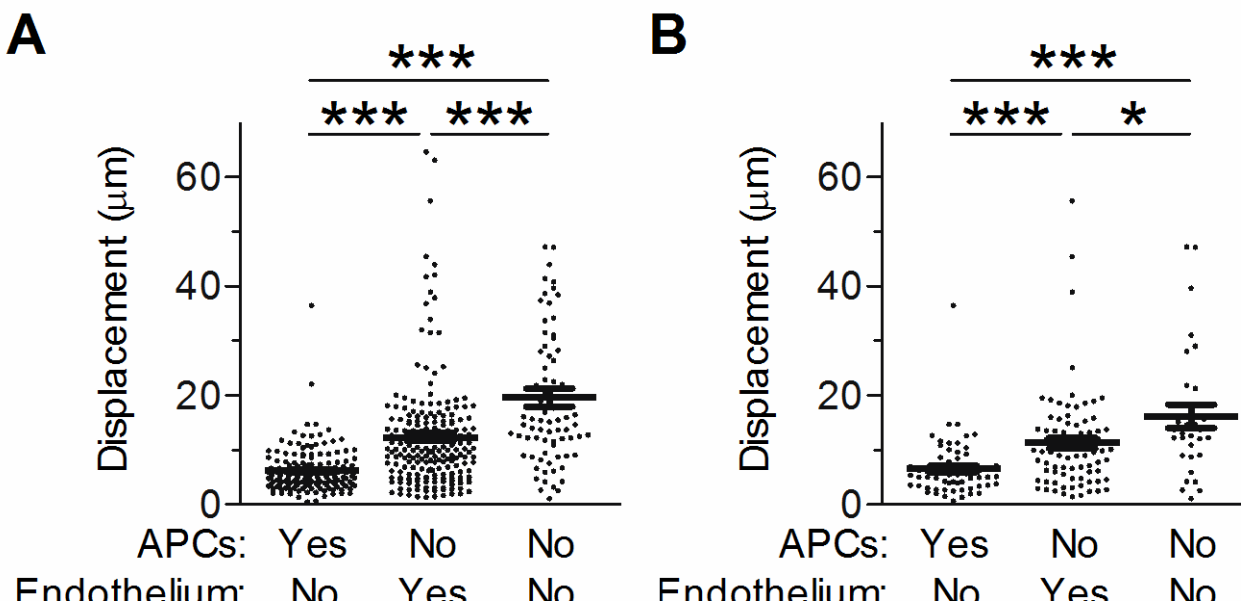

Figure 40. Graft endothelial or APC Ag presentation lowers the displacement of effector T cells.

OT-I effector T cells were transferred into B6-OVA kidney graft recipients 2 days after transplantation. Grafts were imaged by multiphoton intravital microscopy 24 hours after cell transfer and cell tracks are shown in Figure 36. (**A**) Displacement of all OT-I cells tracked in B6-OVA kidney grafts that lack H-2K^b expression on the endothelium (n = 168), APC (n = 206) or both (n = 77). (**B**) Displacement of tracked OT-I cells that remained inside the vascular lumen without transmigrating in B6-OVA kidney grafts that lack H-2K^b expression on the endothelium (n = 65), APC (n = 81), or both (n = 31). Results are mean ± s.e.m.; n.s. = not significant; *p<0.05, **p<0.01, ***p<0.001.

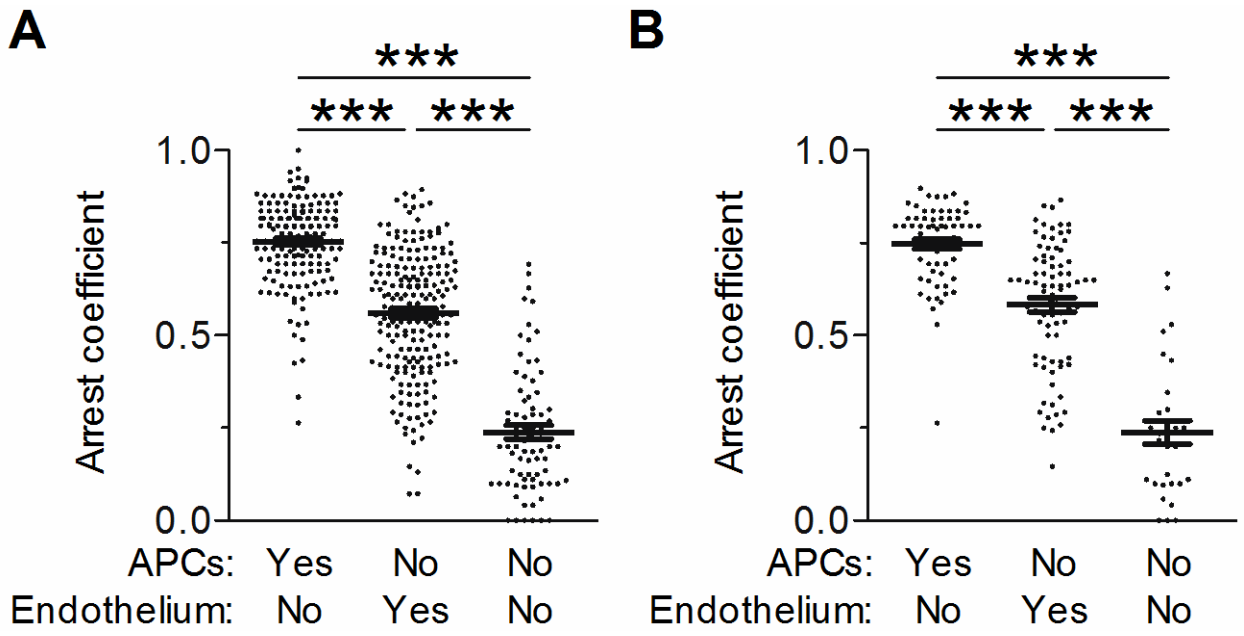

Figure 41. Graft endothelial or APC Ag presentation increases the arrest of effector T cells.

OT-I effector T cells were transferred into B6-OVA kidney graft recipients 2 days after transplantation. Grafts were imaged by multiphoton intravital microscopy 24 hours after cell transfer and cell tracks are shown in Figure 36. (**A**) Arrest coefficient of all OT-I cells tracked in B6-OVA kidney grafts that lack H-2K^b expression on the endothelium (n = 168), APC (n = 206) or both (n = 77). (**B**) Arrest coefficient of tracked OT-I cells that remained inside the vascular lumen without transmigrating in B6-OVA kidney grafts that lack H-2K^b expression on the endothelium (n = 65), APC (n = 81), or both (n = 31). Results are mean ± s.e.m.; n.s. = not significant; *p<0.05, **p<0.01, ***p<0.001.

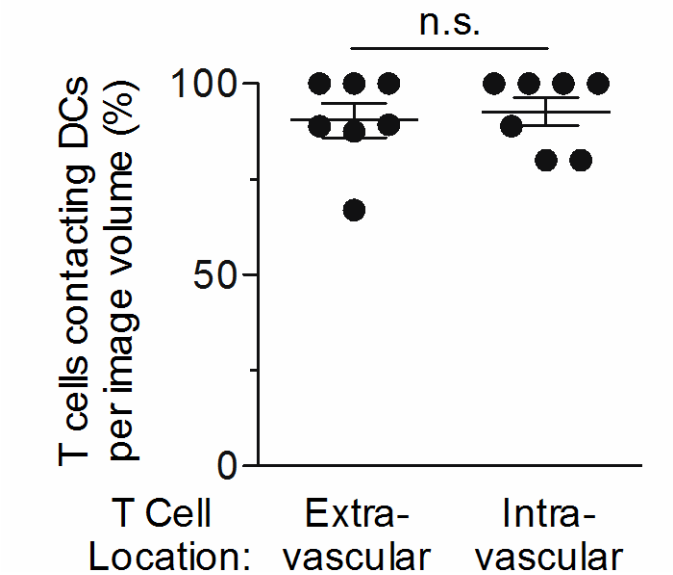

Figure 42. Majority of arrested T cells, irrespective of location, make stable contact with graft DCs.

B6-OVA kidneys that lack H-2K^b expression on the endothelium and in which bone marrow derived dendritic cells (DC) are genetically labeled with YFP were transplanted into B6 recipients with YFP labeled DCs. OT-I effector T cells were transferred to the kidney graft recipients 2 days after transplantation. Grafts were imaged by multiphoton intravital microscopy 24 hours after cell transfer and cell tracks are shown in Figure 36. Graph depicts the percent of OT-I cells making stable contacts with YFP+ DC of B6-OVA kidney grafts (n = 7 movies, 3 independent experiments). Results are mean ± s.e.m.; n.s. = not significant; *p<0.05, **p<0.01, ***p<0.001.

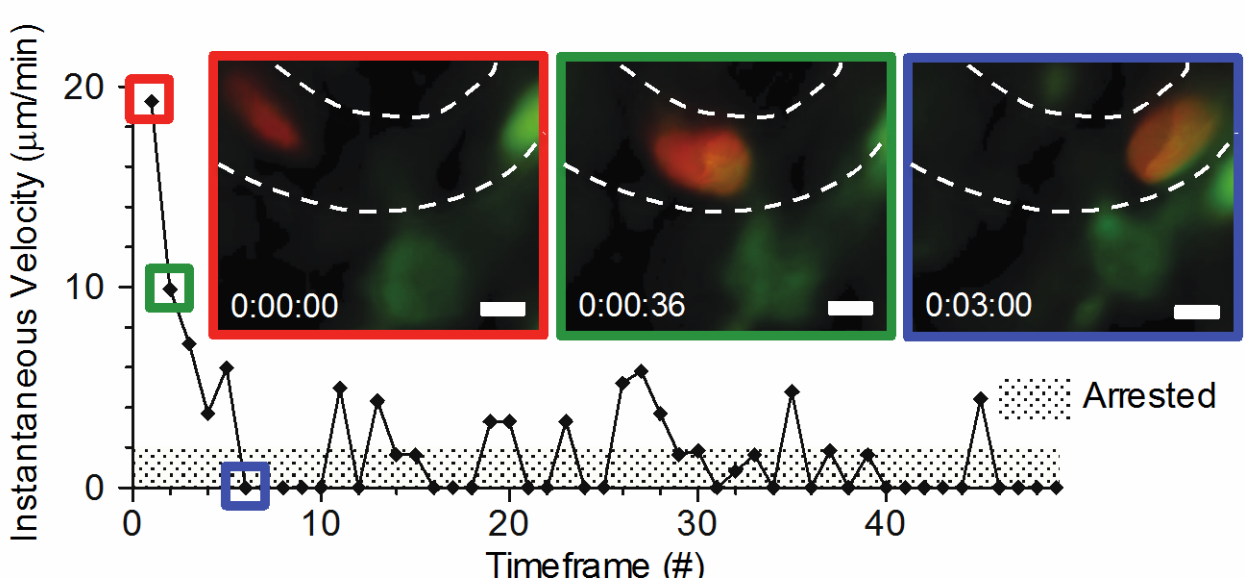

Figure 43. Visualization and instantaneous velocity of OT-I cell arrested after contact with a DC.

Visualization (image panels) and instantaneous velocity (graph) of an OT-I cell (red) arrested in a blood vessel (outlined by dashed line) after making stable contact with a YFP^+ DC (green). B6-OVA kidneys that lack H-$2K^b$ expression on the endothelium and in which bone marrow derived dendritic cells (DC) are genetically labeled with YFP were transplanted into B6 recipients with YFP^+ labeled DCs. OT-I effector T cells were transferred to the kidney graft recipients 2 days after transplantation. Graft was imaged by multiphoton intravital microscopy 24 hours after cell transfer and cell tracks are shown in Figure 36. Scale bars, 5 μm.

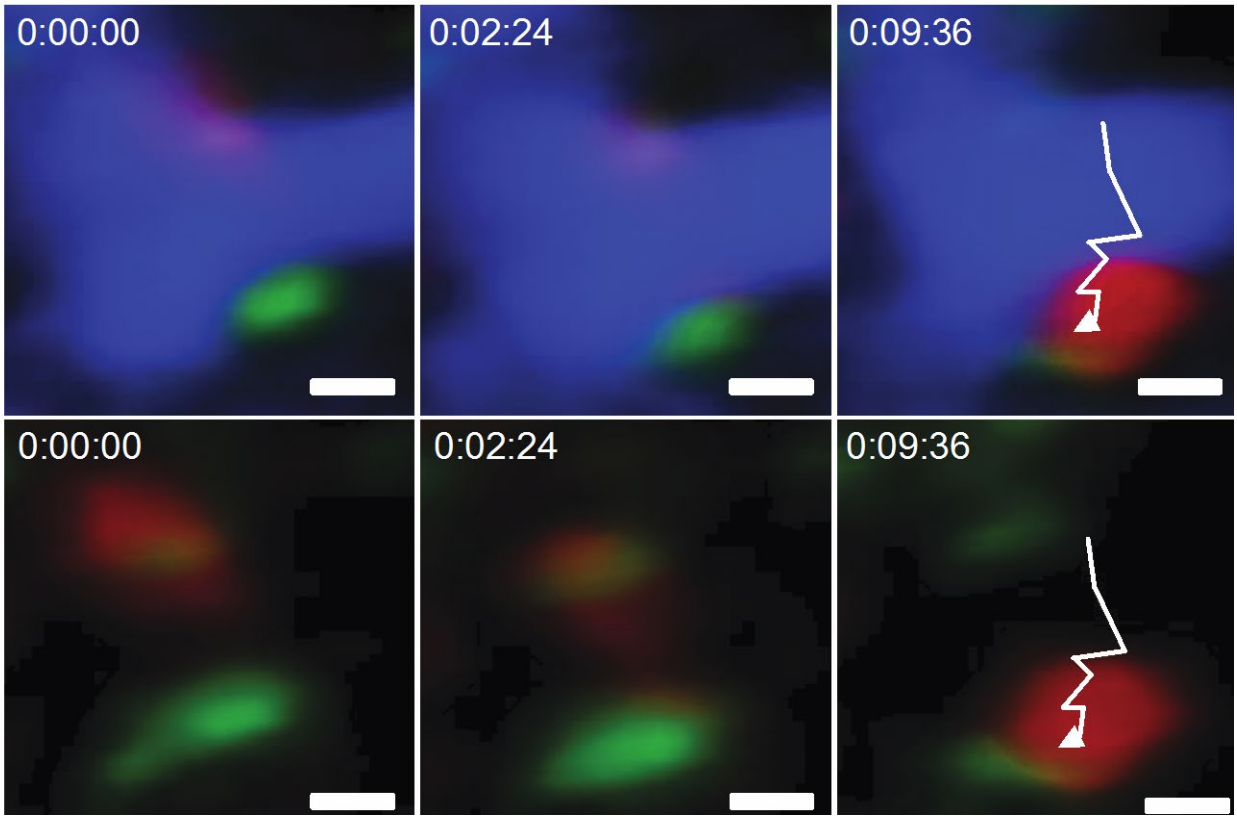

Figure 44. Visualization of an OT-I T cell making stable contact with a DC during transmigration.

Time-lapse images showing an OT-I cell (red) making stable contact with a YFP^+ DC (green) throughout the transmigration process. Blood vessel is labeled in blue and is subtracted in lower panels. B6-OVA kidneys that lack H-$2K^b$ expression on the endothelium and in which bone marrow derived dendritic cells (DC) are genetically labeled with YFP^+ were transplanted into B6 recipients with YFP^+ labeled DCs. OT-I effector T cells were transferred to the kidney graft recipients 2 days after transplantation. Graft was imaged by multiphoton intravital microscopy 24 hours after cell transfer and cell tracks are shown in Figure 36. Scale bars, 5 μm.

4.0 DISCUSSION

4.1 COGNATE ANTIGEN DIRECTS THE MIGRATION OF EFFECTOR T CELLS TO KIDNEY GRAFTS

Our findings shed new light on the pathogenesis of transplant rejection, and more broadly, the immune surveillance of non-lymphoid tissues by $CD8^+$ T cells. We established that a key step in the rejection of transplanted organs, the migration of antigen-specific effector T cells into the inflamed graft, is governed by cognate antigen and not by $G\alpha_i$-dependent chemokine signaling. However, the recruitment of non-specific "bystander" T cells requires both chemokine signaling through the $G\alpha_i$ pathway and the presence of antigen specific $CD8^+$ effector T cells (Figure 45).

The migration of antigen-specific $CD8^+$ T cells to non-lymphoid tissues has been studied previously including: entry into the central nervous system (CNS) through the blood-brain barrier [60], and transmigration through cremasteric venules into the muscle tissue [59]. Experiments in both settings demonstrated that the migration of antigen specific $CD8^+$ T cells into the tissues was directed by presentation of cognate antigen [59, 60]. However, neither group

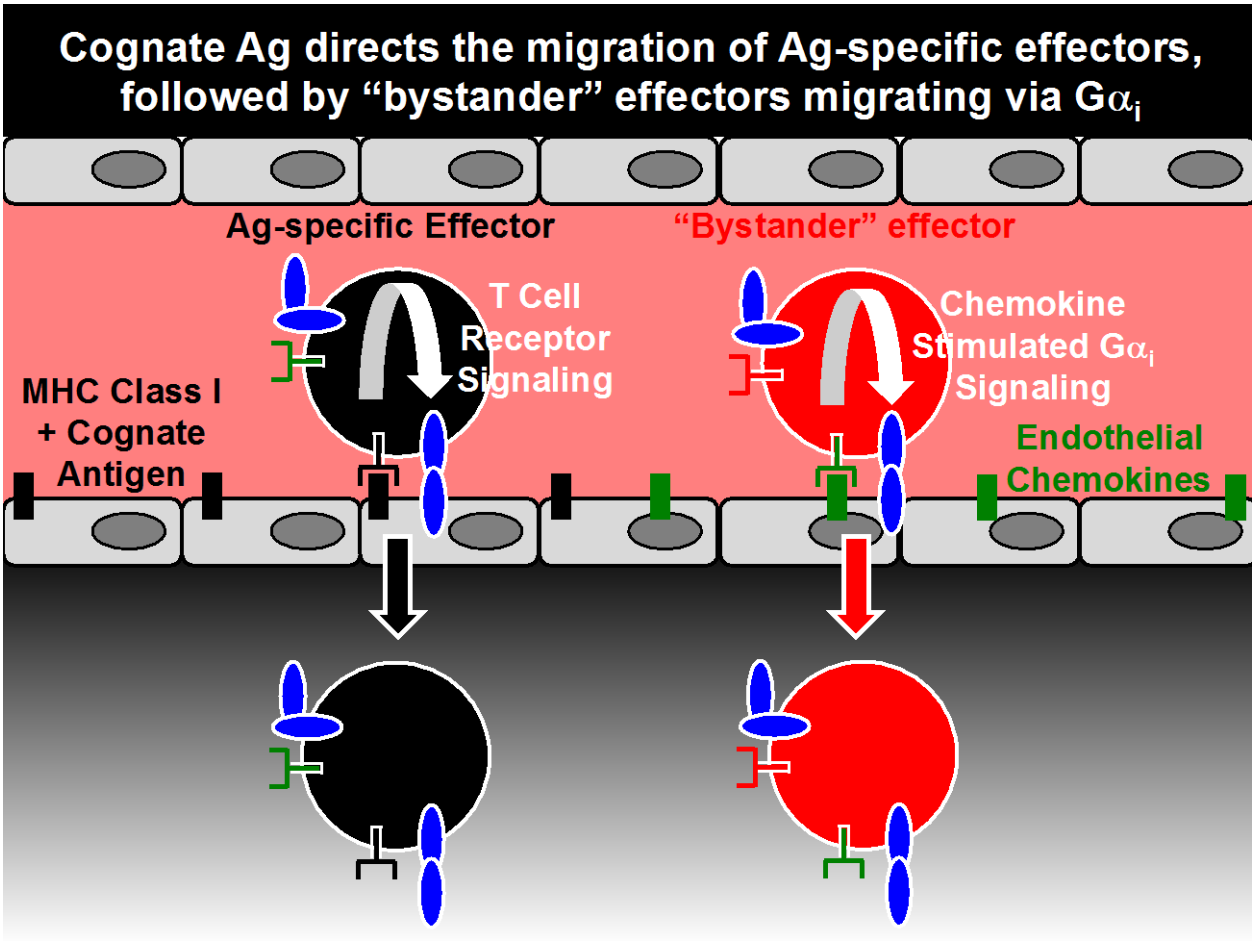

Figure 45. Distinct migratory paradigms for antigen specific versus "bystander" effector T cells.

The migration of antigen-specific $CD8^+$ effector T cells (black circles) into the transplanted organ is governed by cognate antigen (small black rectangles) stimulation of T cell receptor signaling which leads to the expression of high-affinity adhesion molecules (blue ovals) on the cell surface. The migration of antigen-specific $CD8^+$ effector T cells is not governed by $G\alpha_i$-dependent chemokine signaling. However, the recruitment of non-specific "bystander" $CD8^+$ effector T cells (red circles) requires both chemokine signaling through the $G\alpha_i$ pathway and the presence of antigen specific $CD8^+$ effector T cells.

examined the mechanisms of leukocyte adhesion cascade involved in the recruitment of either antigen specific or non-specific "bystander" cells to the respective tissue type. The specific roles of chemokine signaling through the $G\alpha_i$ pathway versus recognition of cognate antigen in both the firm adhesion and transendothelial migration of $CD8^+$ T cells was not investigated in either study.

An analysis of insulin specific T cell migration to the islet of Langerhans in the setting of autoimmune diabetes yielded different results for $CD4^+$ and $CD8^+$ T cells [58, 67, 68]. Early *in vivo* experiments in NOD mice demonstrated that both chemokine stimulated $G\alpha_i$ signaling and antigen recognition through endothelial MHC class I expression were required for insulin-specific $CD8^+$ T cell migration to islets [58]. This is in contrast to the results for antigen specific $CD4^+$ T cell migration that were obtained more recently by another group who utilized both IP-HEL and NOD mice as models of murine autoimmune diabetes [67, 68]. In both murine models of autoimmune diabetes the migration of antigen-specific $CD4^+$ T cells to the islets of Langerhans required the presentation of cognate antigen and occurred independent of chemokine signaling through the $G\alpha_i$ pathway [67, 68]. In contrast, the migration of non-specific $CD4^+$ T cells to the islets of Langerhans required both the presence of antigen-specfic $CD4^+$ T cells and chemokine stimulated $G\alpha_i$ signaling [67, 68]. Taken together, similar to our discovery with respect to $CD8^+$ effector T cell migration to vascularized organ transplants, in the setting of autoimmune diabetes, cognate antigen may direct the infiltration of antigen specific T cells to islets of Langerhans. The presence antigen specific T cells then initiates the resulting immune response involving the entrance of non-specific "bystander" T cells to the islets. However, further study with respect to $CD8^+$ T cells and autoimmune diabetes is required to elucidate the differences between the two groups' findings with respect to each T cell subtype.

Antigen-dependent immune surveillance of non-lymphoid tissues may be advantageous to the host. By restricting the entry of effector or memory T cells to non-lymphoid sites where non-self antigen is present, antigen-dependent T cell migration increases the efficiency by which the antigen is eliminated and at the same time prevents immunopathology in tissues where the antigen is absent.

Our work has provided a greater understanding for the specific roles of chemokine stimulation and cognate antigen recognition in the firm adhesion and transmigration of effector T cells to vascularized allografts. This information may suggest additional therapeutic targets that could be utilized to prolong the survival of life saving organ transplants. New treatment modalities are required because although therapy that blocks the VLA-4 adhesion molecule leads to cardiac allograft prolongation and possible long-term acceptance [81], this treatment has been associated with the development of progressive multifocal leukoencephalopathy (PML), a deadly demyelinating disease of the white matter in the brain [82]. Based on the results of our work, anti-MHC class I monoclonal antibodies could be developed to prevent the presentation of cognate antigen to circulating graft specific effector or memory $CD8^+$ T cells. The efficacy of this treatment modality in reducing the transmigration of effector or memory T cells into graft tissue could be tested *in vivo* utilizing mouse recipients of vascularized organ transplants.

Previous investigations involving the leukocyte adhesion cascade that focused on naïve T cells or utilized either polyclonal effector or memory T cells would not have uncovered distinct migratory paradigms for antigen specific and non-specific “bystander” effector T cells. Naïve T cells have not been primed and initially travel to secondary lymphoid tissues in order to interact with antigen presenting cells, prior to their migration to graft tissue. In contrast, the effector and

memory T cell populations utilized in our experiments migrate directly to organ transplants without the need for priming in the secondary lymphoid tissues.

The use of either polyclonal effector or memory T cells would mask the distinct migratory paradigms for antigen specific versus non-specific "bystander" effector T cells. Utilization of a polyclonal model does not allow for the specific identification of either: (1) the antigen specific T cell subset that migrates in response to the presence of cognate antigen and operates independent of $G\alpha_i$ signaling, or (2) the non-specific "bystander" effector T cells that migrate in response to the presence of antigen-specific T cells and are dependent on $G\alpha_i$ signaling. Due to the small percentage of antigen specific cells within a population of polyclonal effector or memory T cells, treatment with pertussis toxin to block chemokine stimulated $G\alpha_i$ signaling may significantly reduce overall cell migration. However, the inability to distinguish the antigen specific cell population from the non-specific "bystander" population would not allow the investigator to identify the distinct migratory paradigms for both cell subsets. Subsequently, this previously undiscovered primary role for cognate antigen presentation in the migration of effector or memory T cells was not appreciated until the recent use of antigen specific T cells in experimental models.

4.2 EFFECTOR T CELL MIGRATION IS PROMOTED BY ENDOTHELIAL OR APC PRESENTATION OF COGNATE ANTIGEN.

The role of cognate antigen presentation by the endothelium in the migration of T cells has been studied previously at the blood-brain barrier [60], the cremasteric venules [59] and pancreatic islets of Langerhans [58]. However, it has not been determined whether tissue resident bone marrow derived antigen presenting cells direct T cell migration into non-lymphoid tissues.

Dendritic cell projections are capable of penetrating through epithelial and vascular beds and into the lumen of a variety of tissue types [88, 91, 92]. Confocal microscopy analysis of aortic $CD11c^+$ dendritic cells located beneath the endothelium depicted processes that could penetrate endothelial cells and protrude into the lumen [88]. Two-photon microscopy of terminal ileum explants captured rare images of tissue resident dendritic cells that internalized noninvasive *Salmonella* bacterium through processes that extended into the lumen of the small bowel [91]. Similarly, immunofluorescence staining conducted by another group demonstrates that intraepithelial dendritic cells extend projections into the airway lumen [92].

Girard et al demonstrated that dendritic cells controlled the migration of naïve T lymphocytes to lymph nodes by modulating the phenotype of high endothelial venules [93]. Specifically, *in vivo* depletion $CD11c^+$ dendritic cells decreased the firm adhesion and increased the rolling velocity of lymphocytes transiting through the high endothelial venules of peripheral lymph nodes [93]. Microscopy analysis conducted by the Unanue group reveals contact between CD11c-YFP^+ dendritic cells and activated 3A9 T cells that have infiltrated the islets of Langerhans [67]. However, neither study directly proves a role for dendritic cells in the transendothelial migration of lymphocytes. To our knowledge, visualization of bone marrow

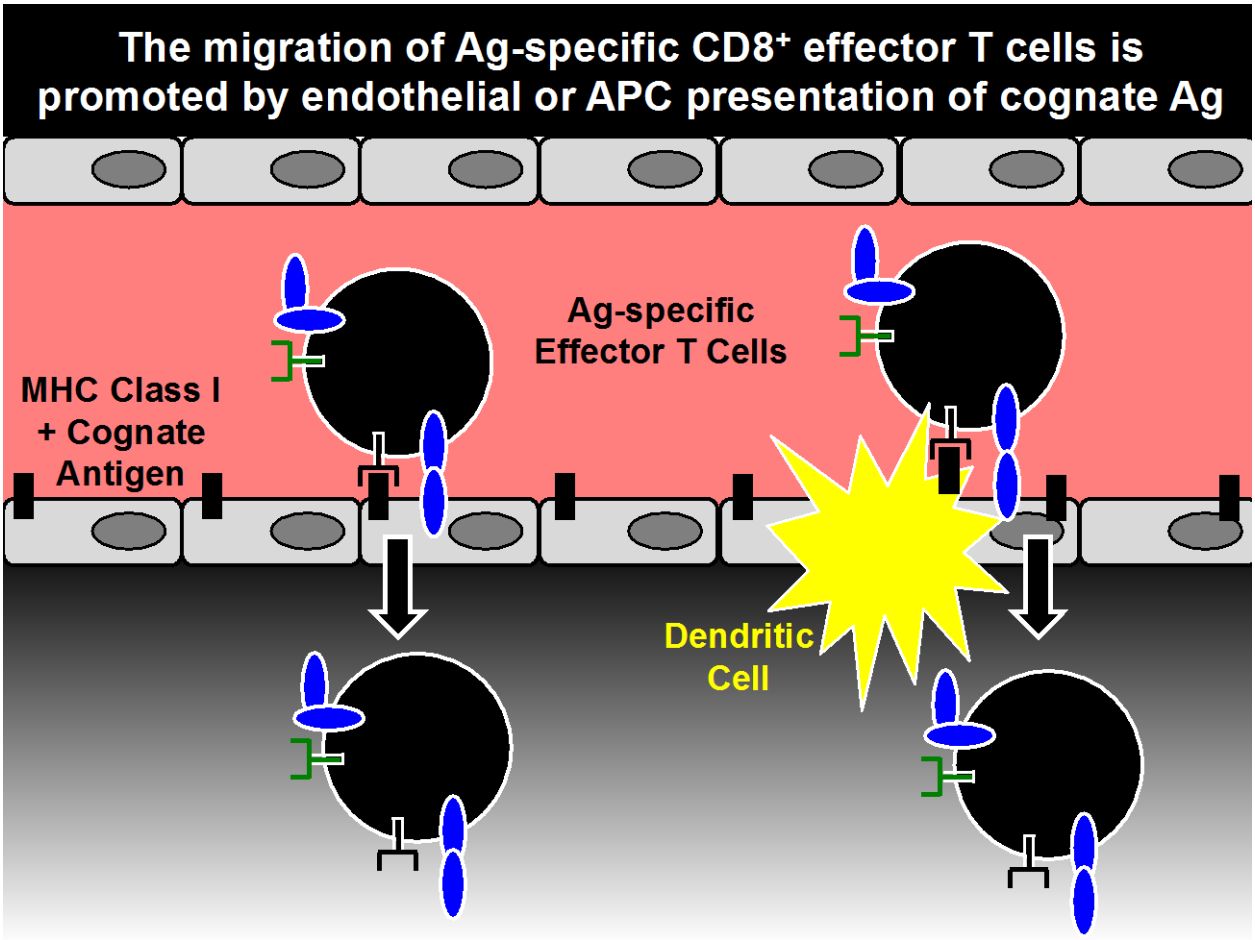

Figure 46. Effector T cell migration is promoted by endothelial or APC presentation of cognate Ag.

The migration of antigen-specific $CD8^+$ effector T cells (black circles) into the transplanted organ is governed by cognate antigen (small black rectangles) stimulation of T cell receptor signaling which leads to the expression of high-affinity adhesion molecules (blue ovals) on the cell surface. Either endothelial or bone-marrow derived APCs (a dendritic cell is presented in yellow) may present cognate antigen and are sufficient to direct the migration of antigen-specific $CD8^+$ effector T cells into the graft.

derived antigen presenting cells directing the transendothelial migration of circulating lymphocytes into the extravascular space has not been presented to date.

Intravital two-photon microscopy that we performed on the transplanted kidney established that antigen presentation by bone marrow derived graft antigen presenting cells is sufficient for arresting effector T cells in the capillary lumen and inducing their transmigration across the capillary wall. This is a previously unappreciated pathway of effector T cell entry into vascularized organ transplants and it sheds new light on the pathogenesis and treatment of rejection. Dendritic cells may become a specific target to prevent allograft rejection due to their role in promoting the migration of effector T cells into transplanted organs. If specific cell surface markers are identified as being expressed by dendritic cells, yet absent from other cell types in organ transplants then those markers could become targets for future therapies aimed at depletion of dendritic cells from allograft tissue.

Antigen presentation by the endothelium is also sufficient to direct the migration of effector T cells into transplanted organs. However, endothelial cells may not be promising targets for ablation therapy to induce tolerance. Targeted depletion of an allograft's endothelial layer may lead to complications and side effects that disrupt the normal physiological functions of the transplanted organ.

The specific roles of both recipient and donor bone marrow derived antigen presenting cells in the transmigration of graft specific effector T cells remain to be determined. Different combinations of chimeric donor kidneys and recipient mice, with or without reconstitution of bone marrow derived antigen presenting cells, could be utilized to determine if any specialization occurs among APCs of donor or recipient origin.

To our knowledge, we present the first visual evidence of tissue resident dendritic cells arresting lymphocytes and maintaining interaction throughout the process transendothelial migration into the extravascular space. This expands the accepted paradigm of the leukocyte adhesion cascade from a focus on cellular interaction with chemokines and ligands presented by the endothelial layer.

APPENDIX A

SUPPLEMENTAL MOVIE LEGENDS

Movies 1 – 3. Time-lapse movies of PTx-treated (red) and untreated (green) OT-I effector cells in an B6-OVA kidney graft (Movie 1) or B6 kidney graft (Movie 2), and of PTx-treated (red) and untreated (green) P14 effector cells in a B6-OVA graft (Movie 3). Blood vessels are labeled in blue. All imaging was performed 24 hrs after cell transfer. 30 second-long z-stacks were repeatedly scanned up to 60 times for a maximum imaging time of 30 minutes. Movies are shown at 10 frames per second.

Movies 4 – 6. Time-lapse movies of OT-I cells (red) in B6-OVA kidney grafts that lack H-2K^{b} expression on the endothelium (Movie 4), APC (Movie 5), or both (Movie 6). Green cells in movie 4 are CD11c-YFP^{+} dendritic cells. Blood vessels in all movies are labeled in blue. Imaging was performed as described for Movies 1 - 3. Movies are shown at 10 frames per second.

Movie 7. Time-lapse movie of an OT-I cell (red) arrested in the blood vessel (cyan) upon making contact with a CD11c-YFP^{+} dendritic cell (green). Imaging was performed as described for Movies 1 - 3. Movie is shown at 3 frames per second.

Movie 8. Time-lapse movie of an OT-I cell (red) making stable contact with a CD11c-YFP^{+} dendritic cell (green) during the transmigration process. Blood vessel is labeled in cyan. Imaging was performed as described for Movies 1 - 3. Movie is shown at 24 frames per second.

BIBLIOGRAPHY

1. Macedo, C., E.A. Orkis, I. Popescu, B.D. Elinoff, A. Zeevi, R. Shapiro, F.G. Lakkis, and D. Metes, *Contribution of naive and memory T-cell populations to the human alloimmune response.* Am J Transplant, 2009. **9**(9): p. 2057-2066.
2. Lakkis, F.G., A. Arakelov, B.T. Konieczny, and Y. Inoue, *Immunologic 'ignorance' of vascularized organ transplants in the absence of secondary lymphoid tissue.* Nature Med., 2000. **6**: p. 686-688.
3. Chalasani, G., Z. Dai, B.T. Konieczny, F.K. Baddoura, and F.G. Lakkis, *Recall and propagation of allospecific memory T cells independent of secondary lymphoid organs. Proc. Natl. Acad. Sci. USA*, 2002. **99**: p. 6175-6180.
4. Obhrai, J.S., M.H. Oberbarnscheidt, T.W. Hand, L. Diggs, G. Chalasani, and F.G. Lakkis, *Effector T cell differentiation and memory T cell maintenance outside secondary lymphoid organs.* J Immunol, 2006. **176**(7): p. 4051-4058.
5. Schenk, A.D., T. Nozaki, M. Rabant, A. Valujskikh, and R.L. Fairchild, *Donor-reactive CD8 memory T cells infiltrate cardiac allografts within 24-h posttransplant in naive recipients.* Am J Transplant, 2008. **8**(8): p. 1652-1661.
6. Springer, T.A., *Traffic signals for lymphocyte recirculation and leukocyte emigration: the multistep paradigm.* Cell, 1994. **76**: p. 301-314.
7. Shulman, Z., V. Shinder, E. Klein, V. Grabovsky, O. Yeger, E. Geron, A. Montresor, M. Bolomini-Vittori, S.W. Feigelson, T. Kirchhausen, C. Laudanna, G. Shakhar, and R. Alon, *Lymphocyte crawling and transendothelial migration require chemokine triggering of high-affinity LFA-1 integrin.* Immunity, 2009. **30**(3): p. 384-396.
8. Kitchens, W.H., D. Haridas, M.E. Wagener, M. Song, A.D. Kirk, C.P. Larsen, and M.L. Ford, *Integrin antagonists prevent costimulatory blockade-resistant transplant rejection by CD8+ memory T cells.* Am J Transplant, 2012. **12**: p. 69-80.
9. Setoguchi, K., A.D. Schenk, D. Ishii, Y. Hattori, W.M. Baldwin, 3rd, K. Tanabe, and R.L. Fairchild, *LFA-1 antagonism inhibits early infiltration of endogenous memory CD8 T cells into cardiac allografts and donor-reactive T cell priming.* Am J Transplant, 2011. **11**(5): p. 923-935.
10. Hancock, W.W., W. Gao, K.L. Faia, and V. Csizmadia, *Chemokines and their receptors in allograft rejection.* Curr. Opin. Immunol., 2000. **12**: p. 511-516.
11. Halloran, P.F. and R.L. Fairchild, *The puzzling role of CXCR3 and its ligands in organ allograft rejection.* Am J Transplant, 2008. **8**(8): p. 1578-1579.
12. Oberbarnscheidt, M.H., J.M. Walch, Q. Li, A.L. Williams, J.T. Walters, R.A. Hoffman, A.J. Demetris, C. Gerard, G. Camirand, and F.G. Lakkis, *Memory T cells migrate to and reject vascularized cardiac allografts independent of the chemokine receptor CXCR3.* Transplantation, 2011. **91**(8): p. 827-832.

13. Game, D.S. and R.I. Lechler, *Pathways of allorecognition: implications for transplantation tolerance.* Transpl Immunol, 2002. **10**(2-3): p. 101-108.
14. Bolton, E.M., J.A. Bradley, and G.J. Pettigrew, *Indirect allorecognition: not simple but effective.* Transplantation, 2008. **85**(5): p. 667-669.
15. Kaplan, B., G.J. Burckart, and F.G. Lakkis, *Immunotherapy in transplantation : principles and practice*. 2012, Chichester, West Sussex, UK: Wiley Blackwell. xi, 459 p.
16. Herrera, O.B., D. Golshayan, R. Tibbott, F. Salcido Ochoa, M.J. James, F.M. Marelli-Berg, and R.I. Lechler, *A novel pathway of alloantigen presentation by dendritic cells.* J Immunol, 2004. **173**(8): p. 4828-4837.
17. Kaech, S.M., E.J. Wherry, and R. Ahmed, *Effector and memory T cell differentiation: Implications for vaccine development.* Nature Reviews Immunology, 2002. **2**: p. 251-262.
18. Hammarlund, E., M.W. Lewis, S.G. Hansen, L.I. Strelow, J.A. Nelson, G.J. Sexton, J.M. Hanifin, and M.K. Slifka, *Duration of antiviral immunity after smallpox vaccination.* Nat Med, 2003. **9**(9): p. 1131-1137.
19. Rogers, P.R., C. Dubey, and S.L. Swain, *Qualitative changes accompany memory T cell generation: Faster, more effective responses at lower doses of antigen.* J. Immunol., 2000. **164**: p. 2338-2346.
20. Adams, A.B., M.A. Williams, T.R. Jones, N. Shirasugi, M.M. Durham, S.M. Kaech, E.J. Wherry, T. Onami, J.G. Lanier, K.E. Kokko, T.C. Pearson, R. Ahmed, and C.P. Larsen, *Heterologous immunity provides a potent barrier to transplantation tolerance.* J Clin Invest, 2003. **111**(12): p. 1887-1895.
21. Adams, A.B., T.C. Pearson, and C.P. Larsen, *Heterologous immunity: an overlooked barrier to tolerance.* Immunol Rev, 2003. **196**: p. 147-160.
22. Valujskikh, A. and F.G. Lakkis, *In remembrance of things past: memory T cells and transplant rejection.* Immunol Rev, 2003. **196**: p. 65-74.
23. Li, Y., X.X. Zheng, X.C. Li, M.S. Zand, and T.B. Strom, *Combined costimulation blockade plus rapamycin but not cyclosporine produces permanent engraftment.* Transplantation, 1998. **66**(10): p. 1387-1388.
24. Mueller, A.R., K.P. Platz, W.O. Bechstein, N. Schattenfroh, G. Stoltenburg-Didinger, G. Blumhardt, W. Christe, and P. Neuhaus, *Neurotoxicity after orthotopic liver transplantation. A comparison between cyclosporine and FK506.* Transplantation, 1994. **58**(2): p. 155-170.
25. Kamar, N., C. Mariat, M. Delahousse, J. Dantal, A. Al Najjar, E. Cassuto, N. Lefrancois, O. Cointault, G. Touchard, F. Villemain, F. Di Giambattista, and P.Y. Benhamou, *Diabetes mellitus after kidney transplantation: a French multicentre observational study.* Nephrol Dial Transplant, 2007. **22**(7): p. 1986-1993.
26. Fischereder, M. and M. Kretzler, *New immunosuppressive strategies in renal transplant recipients.* J Nephrol, 2004. **17**(1): p. 9-18.
27. Cecka, J.M., *The UNOS renal transplant registry.* Clin Transpl, 2001: p. 1-18.
28. Waldmann, H., *Therapeutic approaches for transplantation.* Curr Opin Immunol, 2001. **13**(5): p. 606-610.
29. Klonowski, K.D. and L. Lefrancois, *The CD8 memory T cell subsystem: integration of homeostatic signaling during migration.* Semin Immunol, 2005. **17**(3): p. 219-229.
30. Rose, D.M., R. Alon, and M.H. Ginsberg, *Integrin modulation and signaling in leukocyte adhesion and migration.* Immunol Rev, 2007. **218**: p. 126-134.

31. Ley, K., C. Laudanna, M.I. Cybulsky, and S. Nourshargh, *Getting to the site of inflammation: the leukocyte adhesion cascade updated.* Nat Rev Immunol, 2007. **7**(9): p. 678-689.
32. Carman, C.V. and T.A. Springer, *Integrin avidity regulation: are changes in affinity and conformation underemphasized?* Curr Opin Cell Biol, 2003. **15**(5): p. 547-556.
33. Alon, R. and M.L. Dustin, *Force as a facilitator of integrin conformational changes during leukocyte arrest on blood vessels and antigen-presenting cells.* Immunity, 2007. **26**(1): p. 17-27.
34. Kinashi, T., *Intracellular signalling controlling integrin activation in lymphocytes.* Nat Rev Immunol, 2005. **5**(7): p. 546-559.
35. Bazzoni, G. and M.E. Hemler, *Are changes in integrin affinity and conformation overemphasized?* Trends Biochem Sci, 1998. **23**(1): p. 30-34.
36. Grabovsky, V., S. Feigelson, C. Chen, D.A. Bleijs, A. Peled, G. Cinamon, F. Baleux, F. Arenzana-Seisdedos, T. Lapidot, v.K. Y, R.R. Lobb, and R. Alon, *Subsecond induction of alpha4 integrin clustering by immobilized chemokines stimulates leukocyte tethering and rolling on endothelial vascular cell adhesion molecule 1 under flow conditions.* J Exp Med, 2000. **192**(4): p. 495-506.
37. Constantin, G., M. Majeed, C. Giagulli, L. Piccio, J.Y. Kim, E.C. Butcher, and C. Laudanna, *Chemokines trigger immediate beta2 integrin affinity and mobility changes: differential regulation and roles in lymphocyte arrest under flow.* Immunity, 2000. **13**(6): p. 759-769.
38. Kunkel, E., J. Campbell, G. Haraldsen, J. Pan, J. Boisvert, A. Roberts, E. Ebert, M. Vierra, S. Goodman, M. Genovese, A. Wardlaw, H. Greenberg, C. Parker, E.C. Butcher, D. Andrew, and W. Agace, *Lymphocyte CC chemokine receptor 9 and epithelial thymus-expressed chemokine (TECK) expression distinguish the small intestinal immune compartment: Epithelial expression of tissue-specific chemokines as an organizing principal in regional immunity.* J. Exp. Med., 2000. **192**: p. 761-768.
39. Hudak, S., M. Hagen, Y. Liu, D. Catron, E. Oldham, L.M. McEvoy, and E.P. Bowman, *Immune surveillance and effector functions of CCR10(+) skin homing T cells.* J Immunol, 2002. **169**(3): p. 1189-1196.
40. Koelle, D.M., Z. Liu, C.M. McClurkan, M.S. Topp, S.R. Riddell, E.G. Pamer, A.S. Johnson, A. Wald, and L. Corey, *Expression of cutaneous lymphocyte-associated antigen by CD8(+) T cells specific for a skin-tropic virus.* J Clin Invest, 2002. **110**(4): p. 537-548.
41. Campbell, J.J., G. Haraldsen, J. Pan, J. Rottman, S. Qin, P. Ponath, D.P. Andrew, R. Warnke, N. Ruffing, N. Kassam, L. Wu, and E.C. Butcher, *The chemokine receptor CCR4 in vascular recognition by cutaneous but not intestinal memory T cells.* Nature, 1999. **400**: p. 776-780.
42. Rose, J.R., M.B. Williams, L.S. Rott, E.C. Butcher, and H.B. Greenberg, *Expression of the mucosal homing receptor alpha4beta7 correlates with the ability of CD8+ memory T cells to clear rotavirus infection.* J Virol, 1998. **72**(1): p. 726-730.
43. Gao, W., K. Faia, V. Csizmadia, S. Smiley, D. Soler, J. King, T. Danoff, and W. Hancock, *Beneficial effects of targeting CCR5 in allograft recipients.* Transplantation, 2001. **72**: p. 1199-1205.
44. Hancock, W.W., B. Lu, W. Gao, V. Csizmadia, K. Faia, J.A. King, S.T. Smiley, M. Ling, N.P. Gerard, and C. Gerard, *Requirement of the chemokine receptor CXCR3 for acute allograft rejection.* J Exp Med, 2000. **192**(10): p. 1515-1520.

45. Gao, W., P.S. Topham, J.A. King, S.T. Smiley, V. Csizmadia, B. Lu, C.J. Gerard, and W.W. Hancock, *Targeting of the chemokine receptor CCR1 suppresses development of acute and chronic cardiac allograft rejection.* J. Clin. Invest., 2000. **105**(35-44).
46. Spangrude, G.J., F. Sacchi, H.R. Hill, D.E. Van Epps, and R.A. Daynes, *Inhibition of lymphocyte and neutrophil chemotaxis by pertussis toxin.* J Immunol, 1985. **135**(6): p. 4135-4143.
47. Bargatze, R.F. and E.C. Butcher, *Rapid G protein-regulated activation event involved in lymphocyte binding to high endothelial venules.* J Exp Med, 1993. **178**(1): p. 367-372.
48. Klonowski, K.D., K.J. Williams, A.L. Marzo, D.A. Blair, E.G. Lingenheld, and L. Lefrancois, *Dynamics of blood-borne CD8 memory T cell migration in vivo.* Immunity, 2004. **20**(5): p. 551-562.
49. Murphy, K., P. Travers, M. Walport, and C. Janeway, *Janeway's immunobiology*. 7th ed. 2008, New York: Garland Science. xxi, 887 p.
50. Lim, Y.C., M.W. Wakelin, L. Henault, D.J. Goetz, T. Yednock, C. Cabanas, F. Sanchez-Madrid, A.H. Lichtman, and F.W. Luscinskas, *Alpha4beta1-integrin activation is necessary for high-efficiency T-cell subset interactions with VCAM-1 under flow.* Microcirculation, 2000. **7**(3): p. 201-214.
51. Brezinschek, R.I., P.E. Lipsky, P. Galea, R. Vita, and N. Oppenheimer-Marks, *Phenotypic characterization of CD4+ T cells that exhibit a transendothelial migratory capacity.* J Immunol, 1995. **154**(7): p. 3062-3077.
52. Vajkoczy, P., M. Laschinger, and B. Engelhardt, *Alpha4-integrin-VCAM-1 binding mediates G protein-independent capture of encephalitogenic T cell blasts to CNS white matter microvessels.* J Clin Invest, 2001. **108**(4): p. 557-565.
53. Alon, R., *Encephalitogenic lymphoblast recruitment to resting CNS microvasculature: a natural immunosurveillance mechanism?* J Clin Invest, 2001. **108**(4): p. 517-519.
54. Williams, M.A., A.J. Tyznik, and M.J. Bevan, *Interleukin-2 signals during priming are required for secondary expansion of CD8+ memory T cells.* Nature, 2006. **441**(7095): p. 890-893.
55. Hoyer, K.K., H. Dooms, L. Barron, and A.K. Abbas, *Interleukin-2 in the development and control of inflammatory disease.* Immunol Rev, 2008. **226**: p. 19-28.
56. Feigelson, S.W., V. Grabovsky, E. Winter, L.L. Chen, R.B. Pepinsky, T. Yednock, D. Yablonski, R. Lobb, and R. Alon, *The Src kinase p56(lck) up-regulates VLA-4 integrin affinity. Implications for rapid spontaneous and chemokine-triggered T cell adhesion to VCAM-1 and fibronectin.* J Biol Chem, 2001. **276**(17): p. 13891-13901.
57. Kitani, A., N. Nakashima, T. Izumihara, M. Inagaki, X. Baoui, S. Yu, T. Matsuda, and T. Matsuyama, *Soluble VCAM-1 induces chemotaxis of Jurkat and synovial fluid T cells bearing high affinity very late antigen-4.* J Immunol, 1998. **161**(9): p. 4931-4938.
58. Savinov, A.Y., F.S. Wong, A.C. Stonebraker, and A.V. Chervonsky, *Presentation of antigen by endothelial cells and chemoattraction are required for homing of insulin-specific CD8+ T cells.* J Exp Med, 2003. **197**(5): p. 643-656.
59. Marelli-Berg, F.M., M.J. James, J. Dangerfield, J. Dyson, M. Millrain, D. Scott, E. Simpson, S. Nourshargh, and R.I. Lechler, *Cognate recognition of the endothelium induces HY-specific CD8+ T-lymphocyte transendothelial migration (diapedesis) in vivo.* Blood, 2004. **103**(8): p. 3111-3116.

60. Galea, I., M. Bernardes-Silva, P.A. Forse, N. van Rooijen, R.S. Liblau, and V.H. Perry, *An antigen-specific pathway for CD8 T cells across the blood-brain barrier.* J Exp Med, 2007. **204**(9): p. 2023-2030.
61. Manes, T.D. and J.S. Pober, *Antigen presentation by human microvascular endothelial cells triggers ICAM-1-dependent transendothelial protrusion by, and fractalkine-dependent transendothelial migration of, effector memory CD4+ T cells.* J Immunol, 2008. **180**(12): p. 8386-8392.
62. Schenk, A.D., V. Gorbacheva, M. Rabant, R.L. Fairchild, and A. Valujskikh, *Effector functions of donor-reactive CD8 memory T cells are dependent on ICOS induced during division in cardiac grafts.* Am J Transplant, 2009. **9**(1): p. 64-73.
63. Raab, M., H. Wang, Y. Lu, X. Smith, Z. Wu, K. Strebhardt, J.E. Ladbury, and C.E. Rudd, *T cell receptor "inside-out" pathway via signaling module SKAP1-RapL regulates T cell motility and interactions in lymph nodes.* Immunity, 2010. **32**(4): p. 541-556.
64. Abram, C.L. and C.A. Lowell, *The ins and outs of leukocyte integrin signaling.* Annu Rev Immunol, 2009. **27**: p. 339-362.
65. Dustin, M.L. and T.A. Springer, *T-cell receptor cross-linking transiently stimulates adhesiveness through LFA-1.* Nature, 1989. **341**(6243): p. 619-624.
66. Dustin, M.L., S.K. Bromley, Z. Kan, D.A. Peterson, and E.R. Unanue, *Antigen receptor engagement delivers a stop signal to migrating T lymphocytes.* Proc Natl Acad Sci USA, 1997. **94**(8): p. 3909-3913.
67. Calderon, B., J.A. Carrero, M.J. Miller, and E.R. Unanue, *Cellular and molecular events in the localization of diabetogenic T cells to islets of Langerhans.* Proc Natl Acad Sci U S A, 2011. **108**(4): p. 1561-1566.
68. Calderon, B., J.A. Carrero, M.J. Miller, and E.R. Unanue, *Entry of diabetogenic T cells into islets induces changes that lead to amplification of the cellular response.* Proc Natl Acad Sci U S A, 2011. **108**(4): p. 1567-1572.
69. Camirand, G., Q. Li, A.J. Demetris, S.C. Watkins, W.D. Shlomchik, D.M. Rothstein, and F.G. Lakkis, *Multiphoton intravital microscopy of the transplanted mouse kidney.* Am J Transplant, 2011. **11**(10): p. 2067-2074.
70. Sumen, C., T.R. Mempel, I.B. Mazo, and U.H. von Andrian, *Intravital microscopy: visualizing immunity in context.* Immunity, 2004. **21**(3): p. 315-329.
71. Halin, C., J.R. Mora, C. Sumen, and U.H. von Andrian, *In vivo imaging of lymphocyte trafficking.* Annu Rev Cell Dev Biol, 2005. **21**: p. 581-603.
72. Phan, T.G. and A. Bullen, *Practical intravital two-photon microscopy for immunological research: faster, brighter, deeper.* Immunol Cell Biol, 2010. **88**(4): p. 438-444.
73. Zipfel, W.R., R.M. Williams, and W.W. Webb, *Nonlinear magic: multiphoton microscopy in the biosciences.* Nat Biotechnol, 2003. **21**(11): p. 1369-1377.
74. Centonze, V.E. and J.G. White, *Multiphoton excitation provides optical sections from deeper within scattering specimens than confocal imaging.* Biophys J, 1998. **75**(4): p. 2015-2024.
75. von Andrian, U.H. and T.R. Mempel, *Homing and cellular traffic in lymph nodes.* Nat Rev Immunol, 2003. **3**(11): p. 867-878.
76. Cahalan, M.D., I. Parker, S.H. Wei, and M.J. Miller, *Two-photon tissue imaging: seeing the immune system in a fresh light.* Nat Rev Immunol, 2002. **2**(11): p. 872-880.

77. Germain, R.N., M.J. Miller, M.L. Dustin, and M.C. Nussenzweig, *Dynamic imaging of the immune system: progress, pitfalls and promise.* Nat Rev Immunol, 2006. **6**(7): p. 497-507.
78. Nava, R.G., W. Li, A.E. Gelman, A.S. Krupnick, M.J. Miller, and D. Kreisel, *Two-photon microscopy in pulmonary research.* Semin Immunopathol, 2010. **32**(3): p. 297-304.
79. Cahalan, M.D. and I. Parker, *Choreography of cell motility and interaction dynamics imaged by two-photon microscopy in lymphoid organs.* Annu Rev Immunol, 2008. **26**: p. 585-626.
80. Misgeld, T. and M. Kerschensteiner, *In vivo imaging of the diseased nervous system.* Nat Rev Neurosci, 2006. **7**(6): p. 449-463.
81. Isobe, M., J. Suzuki, H. Yagita, K. Okumura, S. Yamazaki, R. Nagai, Y. Yazaki, and M. Sekiguchi, *Immunosuppression to cardiac allografts and soluble antigens by anti-vascular cellular adhesion molecule-1 and anti-very late antigen-4 monoclonal antibodies.* J. Immunol., 1994. **153**: p. 5810-5818.
82. Bennett, J.L., *Natalizumab and progressive multifocal leukoencephalopathy: migrating towards safe adhesion molecule therapy in multiple sclerosis.* Neurol Res, 2006. **28**(3): p. 291-298.
83. Corry, R.J., H.J. Winn, and P.S. Russel, *Primarily vascularized allografts of hearts in mice: The role of H-2D, H-2K, and non H-2 antigens.* Transplantation, 1973. **16**: p. 343-350.
84. Badovinac, V.P., K.A.N. Messingham, A. Jabbari, J.S. Haring, and J.T. Harty, *Accelerated CD8+ T-cell memory and prime-boost response after dendritic-cell vaccination.* Nat Med, 2005. **11**(7): p. 748-756.
85. Warnock, R., S. Askari, E. Butcher, and U.H. von Andrian, *Molecular mechanisms of lymphocyte homing to peripheral lymph nodes.* J. Exp. Med., 1998. **187**: p. 205-216.
86. Textor, J., A. Peixoto, S.E. Henrickson, M. Sinn, U.H. von Andrian, and J. Westermann, *Defining the quantitative limits of intravital two-photon lymphocyte tracking.* Proc Natl Acad Sci U S A, 2011. **108**(30): p. 12401-12406.
87. Pober, J.S. and G. Tellides, *Participation of blood vessel cells in human adaptive immune responses.* Trends Immunol, 2012. **33**(1): p. 49-57.
88. Choi, J.H., Y. Do, C. Cheong, H. Koh, S.B. Boscardin, Y.S. Oh, L. Bozzacco, C. Trumpfheller, C.G. Park, and R.M. Steinman, *Identification of antigen-presenting dendritic cells in mouse aorta and cardiac valves.* J Exp Med, 2009. **206**(3): p. 497-505.
89. Ouchi, T., A. Kubo, M. Yokouchi, T. Adachi, T. Kobayashi, D.Y. Kitashima, H. Fujii, B.E. Clausen, S. Koyasu, M. Amagai, and K. Nagao, *Langerhans cell antigen capture through tight junctions confers preemptive immunity in experimental staphylococcal scalded skin syndrome.* J Exp Med, 2011. **208**(13): p. 2607-2613.
90. Niess, J.H., S. Brand, X. Gu, L. Landsman, S. Jung, B.A. McCormick, J.M. Vyas, M. Boes, H.L. Ploegh, J.G. Fox, D.R. Littman, and H.C. Reinecker, *CX3CR1-mediated dendritic cell access to the intestinal lumen and bacterial clearance.* Science, 2005. **307**(5707): p. 254-258.
91. Chieppa, M., M. Rescigno, A.Y. Huang, and R.N. Germain, *Dynamic imaging of dendritic cell extension into the small bowel lumen in response to epithelial cell TLR engagement.* J Exp Med, 2006. **203**(13): p. 2841-2852.

92. Jahnsen, F.L., D.H. Strickland, J.A. Thomas, I.T. Tobagus, S. Napoli, G.R. Zosky, D.J. Turner, P.D. Sly, P.A. Stumbles, and P.G. Holt, *Accelerated antigen sampling and transport by airway mucosal dendritic cells following inhalation of a bacterial stimulus.* J Immunol, 2006. **177**(9): p. 5861-5867.
93. Moussion, C. and J.P. Girard, *Dendritic cells control lymphocyte entry to lymph nodes through high endothelial venules.* Nature, 2011. **479**(7374): p. 542-546.